OPEN-FILE REPORT OFR 08-06

Arizona Geological Survey
www.azgs.az.gov

GEOLOGIC MAPPING OF DEBRIS-FLOW DEPOSITS IN THE SANTA CATALINA MOUNTAINS, PIMA COUNTY, ARIZONA

Arizona Geological Survey
Ann Youberg
Michael L. Cline
Joseph P. Cook
Philip A. Pearthree

United States Geological Survey
Robert H. Webb

Geologic Mapping of Debris Flow Deposits in the Santa Catalina Mountains, Pima County, Arizona

Open-File Report 08-06

Ann Youberg
Michael L. Cline
Joseph P. Cook
Philip A. Pearthree
Robert H. Webb

September 2008

Research supported by Pima County Regional Flood Control District, the Arizona Geological Survey, and United States Geological Survey.

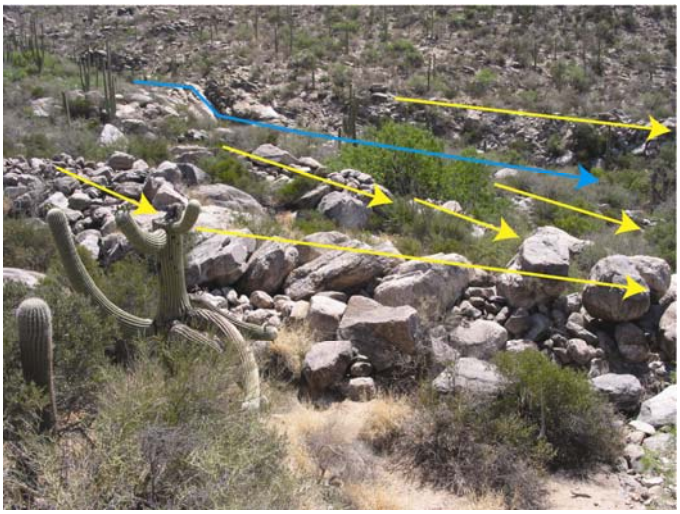

Cover Photo: Debris-flow levees (yellow lines) along Finger Rock Wash (blue line) just downstream of the canyon mouth. Photo taken June 4, 2006, by Ann Youberg.

Suggested Citation:
Youberg, Ann, Cline, M. L., Cook, J. P., Pearthree, P. A., and Webb, R. H., 2008, Geologic Mapping of Debris Flow Deposits in the Santa Catalina Mountains, Pima County, Arizona; Arizona Geological Survey Open-File Report 08-06, 41 pp, 11 map sheets on CD, scale 1:6,000.

Table of Contents

List of Arizona Geological Survey Digital Map Series maps included on accompanying CD:

Map Title	Map Number
Debris-Flow Deposits at the Mouths of Agua Caliente, La Miligrosa, and Molino Canyons	DM-DF-1A
Debris-Flow Deposits at the Mouth of Soldier Canyon	DM-DF-1B
Debris-Flow Deposits at the Mouth of Gibbon Canyon	DM-DF-1C
Debris-Flow Deposits at the Mouths of Bear and Sabino Canyons	DM-DF-1D
Debris-Flow Deposits at the Mouths of Bird and Esperero Canyons	DM-DF-1E
Debris-Flow Deposits at the Mouth of Ventana Canyon	DM-DF-1F
Debris-Flow Deposits at the Mouths of Pontatoc and Finger Rock Canyons	DM-DF-1G
Debris-Flow Deposits at the Mouth of Cobblestone Canyon	DM-DF-1H
Debris-Flow Deposits at the Mouth of Pima Canyon	DM-DF-1I
Debris-Flow Deposits at the Mouth of Pusch Canyon	DM-DF-1J
Debris-Flow Deposits at the Mouth of Linda Vista Canyon	DM-DF-1K

ABSTRACT

An extremely rare weather pattern occurred over southeast Arizona in late July 2006. This five-day storm culminated on July 31, 2006, when the last pulse of precipitation generated record floods in several washes throughout the region, and hundreds of hillslope failures and debris flows in at least four southeastern Arizona mountain ranges. In the Santa Catalina Mountains, debris flows occurred in nine canyons, exiting or nearly exiting the mountain front in five of these canyons. Infrastructure in Sabino Canyon, a popular recreational area, was damaged, as were structures and roads in Soldier Canyon. Historically debris flows in the Santa Catalina Mountains were limited in size, and to upper elevation hillslopes. There are no known reports of debris flows from the Santa Catalina Mountains affecting developed areas in historic times. However, evidence of prehistoric debris flows are present in most canyons and associated alluvial fans along the front range of the Santa Catalina Mountains. While debris flows were previously recognized as significant hazards in Arizona's mountains and canyons , the number and extent of debris flows from the 2006 storm event was surprising.

In order to begin to assess debris-flow hazards along the Santa Catalina Mountains in Pima County, we mapped the extent and character of relatively young prehistoric debris-flow deposits in detail at fifteen canyon mouths. Mapping was conducted on a scale of 1:6,000 using aerial photographs, detailed topography, and field relationships. Deposits were classified into relative age categories based on topographic relationships, soil development and surface characteristics of the deposits. Ages of selected debris-flow deposits in four canyons – Soldier, Sabino, Finger Rock and Pima – were estimated using radiocarbon (^{14}C) and cosmogenic (^{10}Be) isotope methods.

Evidence of past debris flows were found in all fifteen canyons. Relative age dating, corroborated by ^{10}Be, indicates the largest and most extensive deposits in all canyons are late Pleistocene to early Holocene in age. Probable debris-flow deposits of this age are found as much as two miles downstream from the mountain front along several of the larger washes. Younger Holocene debris-flow deposits are much more limited in size and extent, and are found only near the mountain front. Two younger deposits were dated using ^{14}C. A deposit in Finger Rock Canyon was dated to 550 years before present. A deposit in Pima Canyon had a modern date.

Definitive debris-flow recurrence intervals cannot be determined for several reasons. The resolution of age dating, both numerical and relative, is not sufficient to differentiate between deposits. Debris flows are deposited in active channels thus preservation is an issue. Subsequent debris flows or large floods may destroy evidence of previous debris flows through burial or by re-working of the deposits. Existing deposits may be the result of a single debris flow, multiple pulses from a debris flow, or deposition from multiple debris flows separated by an unknown period of time. The relatively limited younger Holocene debris-flow deposits found in all canyons suggest that recurrence intervals for debris flows exiting the Santa Catalina Mountains are probably on the order of thousands of years. Nevertheless, events from 2006 show that some potential exists for debris flows to exit the mountain front into developed areas near canyon mouths.

INTRODUCTION

Background

Debris-flow activity in the Santa Catalina Mountains in July 2006 dramatically illustrated the potential for sizable debris flows to exit canyons along the mountain front and the potential for adverse impacts to properties near canyon mouths. The purpose of this study was to map the extent of prehistoric debris-flow deposits at the mouths of selected Santa Catalina Mountain canyons in eastern Pima County. Arizona Geological Survey (AZGS) geologists mapped the extent of latest Pleistocene to Holocene debris-flow deposits along channels at the mouths of 15 canyons. In late 2007 the scope of work was expanded to include mapping of modern (2006) debris-flow deposits in Soldier Canyon, and to delineate the downstream extent of these deposits in other canyons. United State Geological Survey (USGS) geologists collected wood and rock samples from selected paleodebris-flow deposits to date deposit-ages using radiocarbon and cosmogenic dating techniques. This report summarizes our findings and describes the mapped debris-flow deposits depicted on accompanying map sheets.

Debris flows can be triggered by rare, extreme precipitation events when soils with high antecedent moisture conditions receive prolonged, and sometimes intense precipitation resulting in failure of saturated soil (Anderson and Sitar, 1995; Wieczorek and Glade, 2005). Evidence of geomorphic responses to extreme precipitation events, such as remnant debris-flow deposits, can be found throughout southern Arizona. Potential geologic hazards associated with numerous, coincident debris flows, however, were not fully appreciated prior to July 2006. During the last week of July, southern Arizona experienced five consecutive days of early morning storms generated from monsoonal moisture mixing with a persistent low-pressure system centered over northwestern New Mexico (Magirl and others, 2007). These increasingly wet storms culminated on July 31, 2006, when the last pulse of rain fell on already saturated watersheds. Floods of record occurred in several washes throughout the region, and hundreds of hillslope failures and debris flows were generated in at least four southeastern Arizona mountain ranges (Pearthree and Youberg, 2006). While debris flows were previously recognized as significant hazards in Arizona's mountains and canyons (Wohl and Pearthree, 1991; Melis and others, 1997; Pearthree, 2004), the number and extent of debris flows from the 2006 storm event was unexpected.

Location

The 2006 Santa Catalina Mountain debris flows occurred in response to extreme, prolonged precipitation, with debris flows exiting or nearly exiting the mountains in four southeastern canyons: Soldier, Gibbon, Sabino, and Bird. Canyons farther west along the south side of the Santa Catalina Mountains did not have debris flows, but abundant evidence exists of past debris flows near canyon mouths. AZGS geologists mapped debris-flow deposits at the mouths of all major canyons on the south side of the Santa Catalina Mountains: Agua Caliente, La Milagrosa, Molino, Soldier, Bear, Sabino, Bird, Esperero, Ventana, Pontatoc, Finger Rock, and Pima Canyons (Figure 1). Four smaller, informally named canyons were also mapped: Linda Vista Canyon on the northwest side of Pusch Ridge, Pusch Canyon just west of Pima Canyon, Cobblestone Canyon just west of Finger Rock Canyon, and Gibbon Canyon between Bear and Soldier Canyons. Gibbon Canyon is the only smaller, informally named canyon that had 2006 debris-flow activity.

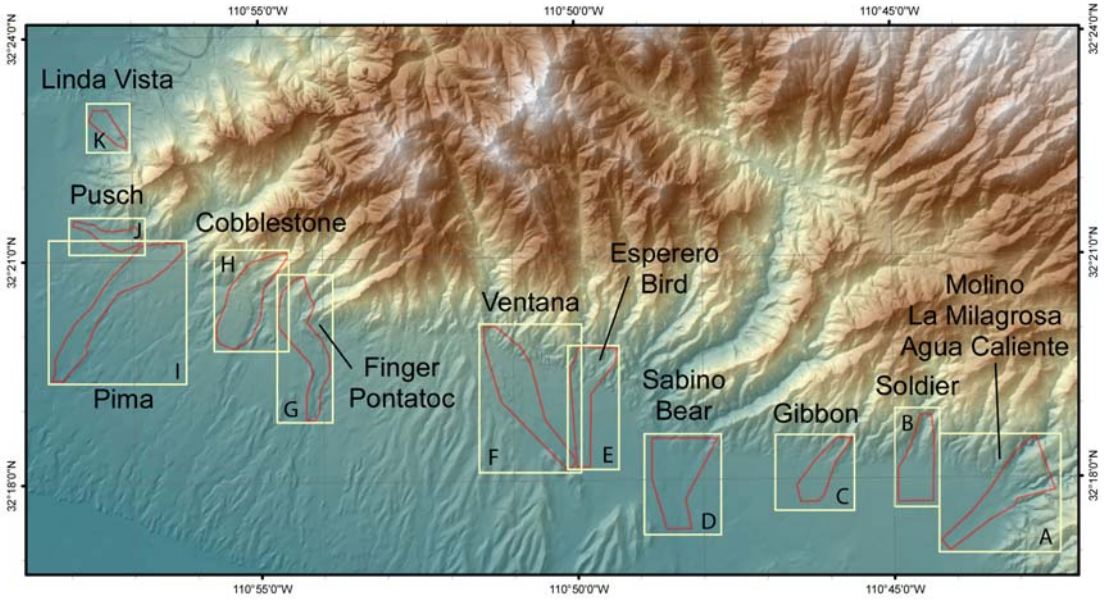

Figure 1. Location of study canyons. Map sheets outlined in yellow; letter corresponds to Digital Map Series Debris Flow Map Number (DM-DF-1_). Maps are included on accompanying CD.

Debris flows

Debris flows are triggered when hillslope soils become saturated and destabilize (De Wrachien, 2006), resulting in mass failure. This typically happens after prolonged or particularly intense rainfall. Debris flows vary widely in size and volume and can be extremely destructive. This section provides a review of debris-flow terminology, initiation, and rheology (deformation and behavior of matter in a flow); and background information with respect to influences of basin characteristics on formation of debris flows.

Terminology

Debris-flow terminology must be carefully defined because of conflicting usages in the literature. Many terminology issues are with respect to classification of flows, and scale of initiating failures and flows. Floods, hyperconcentrated flows, and debris flows are differentiated by sediment concentration and flow rheology (Pierson and Costa, 1987; Pierson, 2005b). Debris flows are sediment-rich slurries at one end of a continuum with water flows (floods) at the other end, and hyperconcentrated flows in the middle. Flood flows typically contain less than 40% sediment by volume and are Newtonian flows (Pierson and Costa, 1987). Suspended sediment in floods consists of clay, silt, and sometimes sand, with gravel generally transported as bedload. Hyperconcentrated flows have around 40-60% sediment by volume and sufficient interaction between grains to keep sediment in suspension as long as flow velocities are maintained (Pierson, 2005b). Deposits from both flood and hyperconcentrated flows exhibit some sorting by grain size (Pierson, 2005a). Debris flows contain more than 60% sediment by volume and consist of sediment-rich fluid matrix and coarse particles. The matrix of a debris flow is composed of clay, silt, and sand in suspension and is driven by high pore pressure. The coarse particles, which are influenced by frictional and gravitational forces, interact with the matrix and each other to prevent particles from settling even at low velocities. Hence, debris-flow deposits exhibit minimal sorting (Iverson and Vallance, 2001; Pierson, 2005b).

The term “mud flow” is sometimes used synonymously with “debris flow” (e.g. Federal Emergency Management Agency, 2008), or to describe a flow with 0-20% coarse clasts and a soft, remoldable clay matrix with high plasticity and liquid limit values (Hungr, 2005). However, the term “mud” has geologic and compositional implications, which is why Pierson and Costa (1987) recommend disregarding the term. Current research describes debris flows as two-phased, non-Newtonian flows dominated by coarse-particle interactions (Iverson, 1997). Thus, use of the term “mud flow” is confusing and unnecessary.

Debris flows can be triggered by different types and sizes of slope failures, often referred to as landslides. Some researchers use the term landslide to describe large, deep-seated rotational or translational mass movements (Glenn and others, 2006), while other researchers apply no scale to the term and use it for all sizes and types of slope failures (Terranova and others, 2007). Shallow landslides are the most common trigger of debris flows (Iverson and others, 1997), especially in areas that have not been subject to recent fire. Generally, the term landslide-induced debris flow is used to describe a shallow translational failure of thin soil over bedrock that liquefies and transforms into a debris flow (Iverson and others, 1997; Cannon and others, 2002; Santi and others, 2007). This description applies to the 2006 debris flows in the Santa Catalina Mountains.

Debris flows have three zones - initiation, transport and deposition - where different processes occur (Hungr, 2005) (Figure 2). Initiation zones are where slope failures occur, usually identified by distinct head scarps, and debris flows are generated. Once initiated, debris flows travel downslope through existing channels. The character of a debris flow changes in time and space as it travels downslope. Debris flows commonly move in surges led by a coarse-boulder front (head), followed by a liquefied slurry (body), and a more watery tail which is often a hyperconcentrated flow (Hungr, 2005). Levees, which confine the flow, may be deposited anywhere along the channel due to longitudinal sorting (Hungr, 2005), but are most obvious in areas with less lateral topographic confinement. Debris-flow volumes can change significantly during downslope movement as scouring or deposition occurs (Iverson and Vallance, 2001). Debris-flow deposition occurs in areas where lateral confinement decreases and/or channel slope decreases. Depositional areas are often alluvial fans located at the mouths of drainages.

Initiation

Hydrological conditions that can trigger debris flows include prolonged or intense convective rainfall (Webb and others, 2005), rain-on-snow events (Meyer and others, 2001; Lenzi, 2006), or rainfall on recently burned areas (Cannon and Gartner, 2005). In Arizona, debris flows have been generated by dissipating tropical storms, prolonged winter storms, intense convective summer storms, and post-wildfire summer storms. Debris flows usually initiate on steep slopes between 20^{o} and 45^{o} (Hungr, 2005) but have initiated on slopes as low as 11° (Lenzi, 2006). Nearly all of the 2006 debris flows in the Santa Catalina Mountains initiated on steep slopes (Webb and others, 2008).

Debris flows in undisturbed (unburned) areas are triggered when soils become saturated and destabilize. Soil pore pressure in saturated soils increases and shear strength decreases to a critical point at which failure occurs, rapidly mobilizing the soil mass into a viscous slurry through liquefaction or dilatancy (Costa, 1984). As described above, the initial failure can be rotational or translational (Costa, 1984). Debris flows can also form in channels when sediments are mobilized by runoff (Costa, 1984). Debris flows formed by mobilized channel sediment, called progressive sediment bulking, have most often been noted following wildfires (Wohl and Pearthree, 1991; Cannon, 2001; Santi and others, 2008).

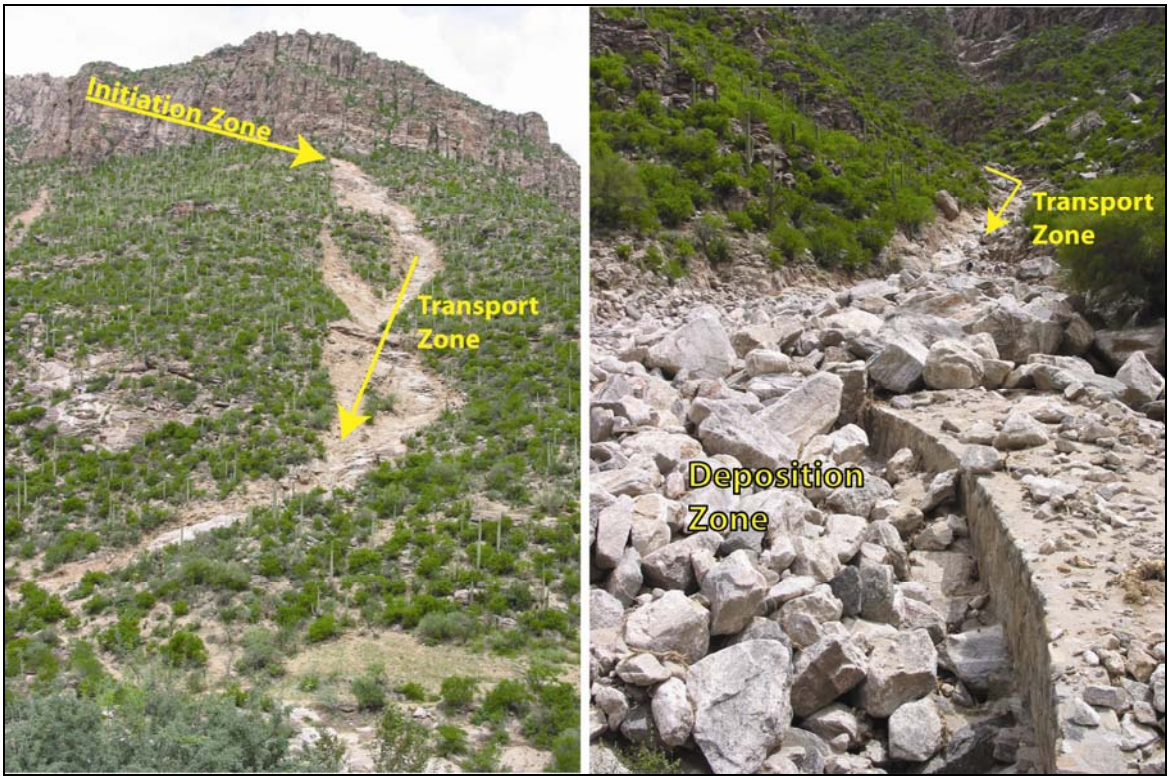

Figure 2. Examples from Sabino Canyon of initiation, transport and deposition zones.

Rheology

Rheology describes the relationship between flow stress and strain rates and how the flow deforms. The seminal work on debris-flow rheology was conducted by Bagnold (1954) in experiments exploring shear and normal stresses in mixtures of non-cohesive, neutrally buoyant grains in a liquid matrix. For many years, based mainly on this work, debris flows were modeled using a single, fixed rheology to describe matrix flow behavior, neglecting the influences of grain-interactions. However, by using non-cohesive, neutrally buoyant grains, Bagnold masked the gravitational forces on grain-to-grain stresses (Takahashi and others, 1997; Iverson and Vallance, 2001). Recent research comparing field observations, laboratory measurements, and numerical modeling show debris flows with significant amounts of coarse clasts can not be sufficiently modeled using a one-phase rheology approach, regardless of matrix clay content (Sosio and others, 2007). Data show grain-to-grain interactions of coarser material in an interstitial fluid are best represented by a two-phase granular approach where both pore pressure and frictional effects are represented (Sosio and others, 2007). Most researchers now view debris flows as a two-phased flow composed of a finer-grained matrix influenced by pore pressure and a coarse-grained fraction influenced by frictional and gravitational forces (Iverson, 1997; Takahashi and others, 1997; Iverson and Vallance, 2001; Sosio and others, 2007).

Instead of rheological equations, Iverson and Vallance (2001) use the Coulomb equation to describe flow behavior. This equation has no dependence on stress rate, but maintains proportionality between shear and normal stresses while satisfying conservation of momentum (Iverson and Vallance, 2001). Grain-fluid mixtures have unsteady flow characteristics due to fluctuating states, which affects flow patterns.

The flow tends to move as a rigid plug-like flow if pore-pressure and intergranular interactions are low and is more fluid-like when these variables are high (Iverson and Vallance, 2001). Both pore pressure and granular interactions change as the debris flow moves downslope. As a result, flow depth fluctuates to accommodate volumetric changes due to the affects of grain-to-grain interactions and variable pore-pressure (Iverson and Vallance, 2001). These unsteady flow characteristics can be seen in the anatomy of a debris flow. The abrupt, coarse-grained surge head, dominated by Coulomb friction, is followed by a more fluid body and tail with fluctuating pore-fluid pressure and intergranular stresses (Iverson and Vallance, 2001).

GIS-Derived Basin Characteristics

Many models have been developed to assess debris-flow behavior (Iverson, 1997; Iverson and others, 2005), to estimate debris-flow erosion (Stock and Dietrich, 2006), and to predict debris-flow hazards (O'Brien and others, 1993; Wilford and others, 2004; Cannon and Gartner, 2005; Gartner and others, 2005). These models address debris flows generated from extreme precipitation, rapid snow melt, or as a result of disturbance due to land-use change, such as logging or wildfires. Many models use basin morphometric parameters (basin size, shape, and gradient) to evaluate the probability of debris-flow occurrence and potential volume of material generated (Wilford and others, 2004; Gartner and others, 2007).

Basin morphometric parameters are a function of basin contributing area, basin relief, hillslope processes, geology, and climate (Tucker and Bras, 1998; Wohl, 2000). Basins with higher relief and higher-gradient streams have more capacity to transport larger clasts and typically have greater quantities of available sediment than low-relief basins with lower-gradient streams (Montgomery and Buffington, 1997). Recent work suggests that basin area, average basin gradient, aspect, relief ratio, Melton Ratio, and length of watershed are potential indicators of debris-flow prone basins (Wilford and others, 2004; Cannon and Gartner, 2005; Rowbotham and others, 2005). The relief ratio and Melton Ratio are both measurements of basin ruggedness. The relief ratio describes basin topographic relief with respect to the length of the watershed: the Melton Ratio describes basin relief with respect to the square root of basin area. While modeling and basin analysis were not part of this study, and all mapped canyons have evidence of past debris-flow activity, a brief examination of basin and channel morphometrics from the study canyons may provide insight regarding potential basin response to a given rainfall sequence.

METHODS

GIS-Derived Basin Characteristics

Basin and stream measurements were derived using ESRI ArcMap 9.2 spatial analysist and an ArcMap extension called Terrain Analysis Using Digital Elevation Models (TauDEM) (Tarboton, 2005). GIS tools extract basin measurements such as area, elevation, orientation, slope gradient, and basin length. Stream networks were derived for each canyon using TauDEM, which calculates flow direction and accumulation for each cell in a digital elevation model (DEM). The user selects a threshold flow accumulation value to extract stream networks. For example, a threshold flow accumulation value of 100 means that for any given cell to become part of the stream network at least 100 upslope cells must drain into that cell. Several methods have been developed to select appropriate threshold values for stream network extraction from a DEM (Tucker and others, 2001; Tarboton, 2005). One accepted

method, used in this study, is to select values using trial and error to derive a network as similar as possible to printed USGS topologic maps (scale 1:24000) (Tarboton, 2005). Stream networks were derived using an accumulation threshold of 1000 cells; an area slightly less than 25 acres. The derived stream network shapefile was imported into a geodatabase and placed into a geometric framework, using ArcGIS tools, to extract stream profiles and calculate average stream gradients.

Basin and channel morphometric parameters were derived from a single outlet point for each study canyon. Outlet points were created and entered into a GIS point shapefile by selecting a stream network cell where the wash exits the mountain front. The basin consists of all upslope cells that drain through the outlet point.

Geologic Mapping of Debris-Flow Deposits

Debris-flow deposits were mapped using a combination of 1960 (scale 1:9,000) and 2007 (scale 1:12,000) black-and-white aerial photographs from Cooper Aerial Surveys; 2002 Pima County color digital orthophoto imagery; and extensive field observations. Each canyon was walked as far downstream as debris-flow or likely debris-flow deposits were encountered, although in some areas development has masked or substantially modified debris-flow deposits. Debris-flow deposits were also mapped well upstream of the Coronado National Forest boundary. Field observations were recorded with GPS coordinates (several meter positional uncertainty), digital photographs, and notes. ESRI ArcMap GIS software was used to combine field data and aerial photographic information to delineate debris-flow deposits as accurately as possible at a scale of 1:6,000.

Debris-flow deposits were differentiated by relative age using topographic relationships, surface characteristics of boulders, and soil characteristics. Multiple generations of relatively young (Holocene to latest Pleistocene) debris-flow deposits exist in each drainage, but the number of separate debris-flow deposits mapped represents a minimum number of debris flows for several reasons:

- Each mapped deposit may have formed as a result of multiple pulses from single flow or numerous successive debris flows.
- Not all Holocene debris-flow deposits are preserved due to the active nature of the channel environment and erosion and deposition in subsequent debris flows.
- Many debris-flow deposits are likely overlain by more recent deposition and are not visible at the surface (Figure 3).
- Bouldery sections of the channel can be attributed to either reworked debris-flow sediments or heavily eroded debris-flow lobes.

Relative ages of debris-flow deposits were estimated using soil characteristics when present, weathering characteristics of large clasts (boulders and cobbles), and position in the landscape (Birkland, 1999; Menges and others, 2001). Clasts in older debris-flow deposits generally exhibited darkened weathering rinds, some degree of oxidation (orange surface patina), fracturing and splitting, and in some deposits, slight to moderate burial. In contrast, clasts in younger deposits had no weathering rinds and weak to non-existent surface patinas, and thus were brighter and fresher looking, with little to no soil accumulation or fracturing.

The general labeling scheme used to place mapped debris-flow deposits in relative age order is described below. Debris-flow deposits cannot be directly correlated between canyons as we do not have sufficient age control, but various deposits in each canyon were classified by estimated age. Numbers

indicate levels of relative age distinctions between debris-flow deposits of broadly similar ages. The generalized labeling scheme presented below was modified as needed for each canyon.

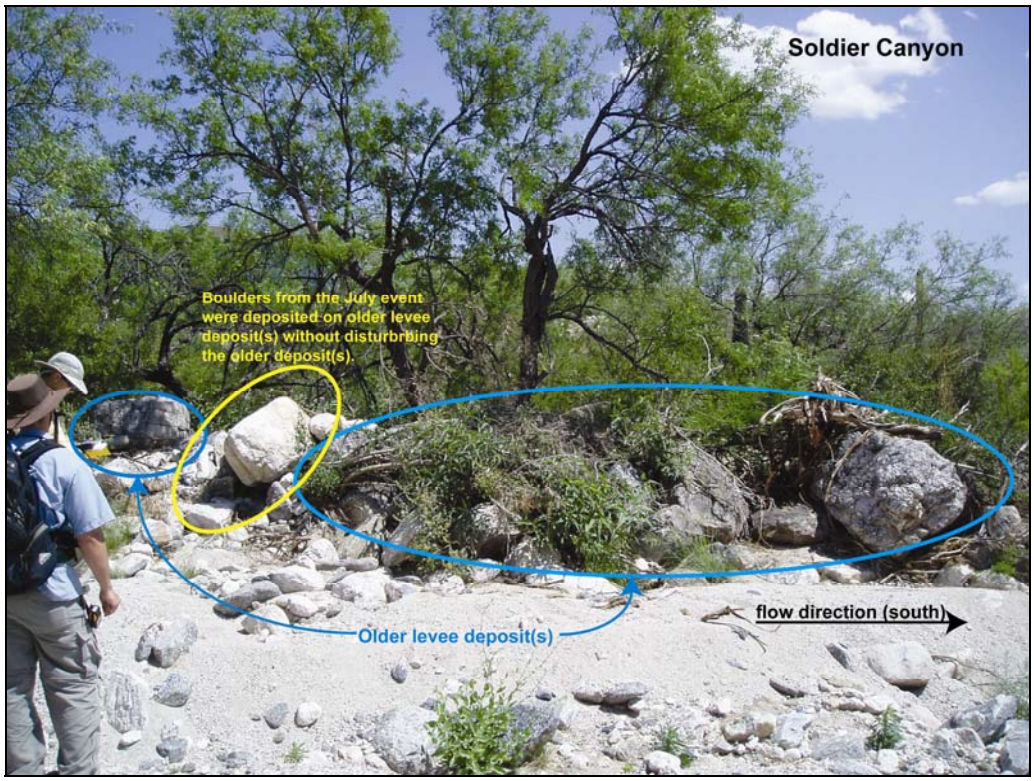

Figure 3. An example from Soldier Canyon of fresh 2006 debris-flow deposits (yellow circle) overlying older undisturbed deposits (blue circles).

Debris-flow deposits often exhibit characteristic morphology based on depositional processes. Levees are linear aggregations of boulders and cobbles that form along lateral margins of debris flows during downslope transport (Figure 4). Snouts are wider, lobate aggregations of boulders and cobbles that form where debris flows terminate (Figure 5). When characteristic morphology was identified during field mapping or through aerial photographic interpretation, debris-flow deposits were classified as either levee (subscript L) or snout (subscript S). Deposits of uncertain morphology, due to either partial burial or disturbance, were undifferentiated (no subscript L or S). Two other types of coarse cobble- and boulder-dominated deposits, found some distance from the mountain front, were also classified based on morphology. Boulder-bar (B) deposits exhibited some debris-flow characteristics but could not be clearly identified to due to partial burial or disturbance of deposits. Coarse, unsorted cobble and boulder (C) deposits were exposed along channel banks bottoms, and interpreted as older debris-flow deposits reworked by either high discharge fluvial processes or secondary debris flows. Both B and C deposits were found at the lower extent of mapped debris-flow deposits. Many of the areas mapped have been disturbed to some degree by development. In some areas older debris-flow deposits evident in earlier aerial photographs have been obscured by recent development.

Figure 4. An example of a well-preserved levee deposit in Esperero Canyon. This deposit was mapped as unit YI (see text below).

Figure 5. An example of a well-preserved snout deposit from Pima Canyon. This deposit was mapped as Y1 (see text below).

Generalized Map Unit Descriptions

In deposits that are identifiable as either levees or snouts, the type of deposit denoted by subscript letter:

L = Debris-flow levees
S = Debris-flow snouts

Preliminary age estimates for various deposits, from oldest to youngest, are in parentheses. Soils colors are based on the Munsell Soil Color Chart.

I – Pleistocene debris-flow deposits, undifferentiated. Debris-flow deposits that are either the highest, most weathered deposits in the landscape and have clearly reddened soil (5YR), or are indurated deposits that have been buried by younger debris flows and exposed through subsequent erosion.

YI- Older debris-flow deposits (latest Pleistocene to early Holocene). Debris-flow deposits that are spatially removed from active fluvial systems, either high-standing or laterally separate from younger deposits. Clasts are slightly to moderately weathered, lightly to moderately stained by oxidation, and commonly exhibit fracturing and splitting. Surfaces between boulders are slightly reddened (7.5YR), and in some areas clasts are partially to almost completely buried by finer deposits. Clasts from disturbed deposits often have thin, discontinuous carbonate coatings. In some areas YI deposits can be further classified into two levels:

YI_1 - Highest standing debris-flow deposits.
YI_2 - Debris-flow deposits of similar age inset 3-7 feet (ft [1-2 m]) below YI_1 deposits.

Y1 – Intermediate debris-flow deposits (early to middle Holocene). Debris-flow deposits found 7-10 ft (2-3 m) above active washes near the mountain front and 3-7 ft (1-2 m) above the active washes farther away from the mountain fronts. Y1 deposits typically are fairly extensive on the upper portions of fans, but are confined to valley bottoms along incised drainages farther out from the mountain front. Clasts generally are slightly weathered, with light surface oxidation and little rock fracturing. Clasts in Y1 deposits may be slightly buried from initial deposition and subsequent abandonment, soil accumulation, or overbank deposition. Soil color varies from gray (10YR) to brown (7.5YR).

Y2 – Young debris-flow deposits (middle to late Holocene). Debris-flow deposits found along banks and terraces of active washes, typically 3-7 ft (1-2 m) above channel floors (Figure 6). Fine grained matrix sediments are generally absent from Y2 deposits leaving only clasts that appear fresh and unweathered. Vegetation typically is sparse on boulder levees and snouts, but deposits generally have some mature vegetation growing in them.

Y3 – Very young debris-flow deposits (latest Holocene to modern). Debris-flow deposits found in and adjacent to active channels near the mountain front and on upper portions of active alluvial fans (Figure 7). Clasts are fresh and unweathered. Vegetation typically is sparse on boulder levees and snouts. Y3 deposits are commonly located in or immediately adjacent to stream channels and are subject to reworking by fluvial processes, so the extent and characteristics of deposits may change with successive flow events.

Y4- Modern debris-flow deposits (2006). Debris-flow deposits in Soldier Canyon emplaced in 2006 (Figure 8). The decision to map these modern deposits occurred in late 2007, after significant channel alterations occurred on Soldier fan adjacent to the Mount Lemmon Short Road. The location and extent

of the 2006 debris-flow deposits adjacent to the Mount Lemmon Short Road are based mainly on photographs taken by the USGS and AZGS in August and September of 2006. Deposits denoted with a question mark (Y4?) have debris-flow characteristics but may be flood-related or re-worked.

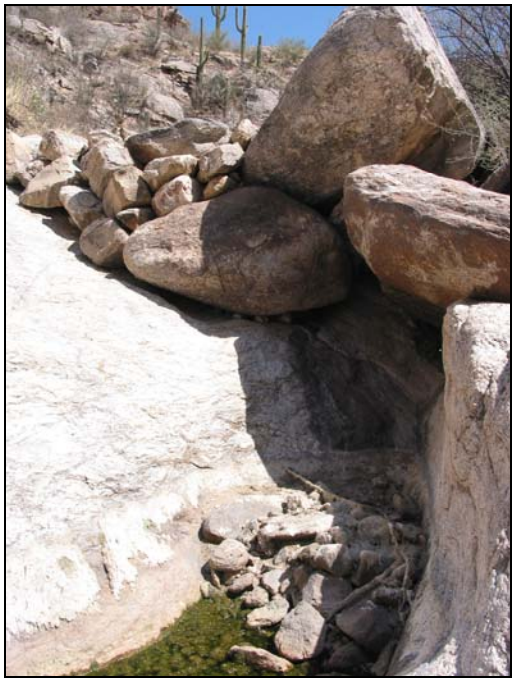

Figures 6 and 7. Figure 6 (left) An example of a boulder levee (unit Y2) from Linda Vista canyon. Figure 7 (right) An example of a debris-flow deposit (unit Y3) in Pontatoc Wash.

Figure 8. 2006 debris-flow deposits in Soldier Wash upstream of the Mount Lemmon Short Road. Yellow lines highlight boulder snout deposited after, and on top of, an earlier pulse that likely plugged the bridge. Blue arrows show direction of flow. Photo: P.G. Griffiths, Sept. 12, 2006 (see Solder Canyon discussion below).

B – Boulder-bar deposits. Elongate cobble and boulder dominated deposits. B deposits resemble debris-flow levees but are often partially buried or possibly reworked by fluvial processes (Figure 9). B deposits are often inundated by fine sediments either from initial deposition and subsequent abandonment, soil accumulation, or overbank deposition. B deposits were used to define downstream extent of paleo-debris-flow deposits in several canyons.

Figure 9. An example of a boulder deposits (unit B) in Pima Canyon, south of Ina Road.

C – Coarse cobble and boulder deposits. Coarse cobble and boulder dominated deposits derived from reworked debris-flow deposits. Found in channel bottoms or forming channel banks (Figure 10). These deposits generally do not exhibit sorting when viewed in channel banks, but also do not exhibit defining debris-flow deposit characteristics. C deposits probably represent winnowed and reworked debris-flow deposits by fluvial processes.

Figure 10. An example of a C deposit in Pima Wash south of Ina Road. Note carbonate coatings. Some C deposits had clasts with carbonate coatings while others did not. Some carbonate coatings are probably a result of shallow ground water and may not be a reliable indicator of age.

Numerical Age Dating of Debris-Flow Deposits

Radiocarbon Dating

We used ^{14}C (radiocarbon) dating techniques to determine ages for recent debris flows in Finger Rock and Pima Canyons. ^{14}C is a radioactive isotope of carbon that is produced in the atmosphere from cosmogenic spallation reactions with ^{16}O and ^{14}N (Gosse and Phillips, 2001). ^{14}C accumulates in living material in equilibrium with atmospheric ^{14}C concentrations through respiration and absorption of CO_2 (plants) or consumption of organic material containing ^{14}C (animals). Beginning with the advent of above-ground testing of hydrogen bombs in 1952, production rates for ^{14}C in the atmosphere greatly increased, providing the tool of post-bomb ^{14}C ages that potentially are accurate to months (Ely and others, 1992); at present (2008), production rates of ^{14}C are essentially at pre-testing levels, although burning of fossil fuels dilutes the atmospheric concentration of ^{14}C with stable ^{12}C and ^{13}C atoms. ^{14}C has a half-life of about 5,200 years and has long been used for age dating of geologic deposits bearing organic material that was deposited in association with sediments (Libby and others, 1949). The organic material collected for ^{14}C age dating was found in association with debris-flow deposits, either as fine twigs trapped between boulders in such a way as they could only have been transported in the debris flow, or plants that were killed and trapped in debris-flow deposits. All sample preparation and analyses were performed at Geochron Laboratories in Billerica, Massachusetts, using standard techniques (http://www.geochronlabs.com/14c.html).

Cosmogenic Dating

Numerous cosmogenic isotopes are produced in rocks and minerals exposed at the Earth's surface (Gosse and Phillips, 2001). For quartz-rich rocks, such as granites in the Santa Catalina Mountains, the typical isotopes used for cosmogenic dating are beryllium (^{10}Be) and aluminum (^{26}Al). Because this type of rock typically has a high, non-cosmogenic aluminum content but essentially no beryllium content (Gosse and Phillips, 2001), we excluded ^{26}Al from our measurements of latest Pleistocene and Holocene debris-flow deposits.

We used cosmogenic dating of debris-flow deposits to attempt to verify and expand the relative age-dating assessments. This technique has long been used to date debris-flow deposits, which are difficult to numeric age-date otherwise (Bierman and others, 1995; Cerling and others, 1999; Webb and others, 1999). Cosmogenic dating, in its simplest usage, reflects the amount of time a rock or mineral has been exposed at the Earth's surface to cosmic ray bombardment. Cosmogenic rays penetrate rocks to a depth of about 3 ft (1 m) for measurable production of most cosmogenic isotopes, and the production rate decays in an approximate exponential fashion with depth; rocks below 7 ft (2 m) depth are essentially shielded from cosmic rays and have negligible production of cosmogenic isotopes prior to debris-flow transport and exposure at the debris-flow surface. For all depths, muon emissions are an important source of ^{10}Be and can be more than 4% of the total production rate; however, this source of ^{10}Be can be corrected easily (Balco and others, 2008). The total concentration of a cosmogenic nuclide (i.e., ^{10}Be) in a rock/mineral is a combination of ^{10}Be accumulated since emplacement of the rock in a landform of interest (i.e., a debris-flow deposit) plus any ^{10}Be that may have accumulated in the rock before deposition in the new landform. One of the key assumptions in using cosmogenic dating as a numerical dating technique is that any sampled rock is either assumed to have been shielded (no prior exposure history). Corrections can be made using depth profiles and/or amalgamation samples to correct inherited nuclide from a prior exposure history (e.g., Anderson and others, 1996; Wolkowinsky and

Granger, 2004). Thickness of the sample, as well as its shielding from low-angle cosmic rays by nearby rocks or cliffs, is an important value for converting an isotopic concentration to a surficial age.

Cosmogenic ^{10}Be, a radioactive isotope with a useful lifetime of 2.2 million years, is dominantly created by spallation reactions resulting from cosmic-ray collisions with either ^{28}Si or ^{16}O in a quartz molecule (SiO_2). The production rates of ^{10}Be atoms in quartz range from 4.74 to 6.4 atoms/g/yr when normalized to high latitude and sea level with various scaling methods (Gosse and Phillips, 2001) Production rates vary with elevation, latitude, and longitude; in particular, they increase with elevation and latitude. Longitude helps locate the samples geographically, so as to account for variations in atmospheric pressure; if in place over long periods of geologic time, low pressure weather systems increase production rates (Balco and others, 2008). An on-line calculator developed for the CRONUS-Earth project is useful for estimating the production rate of ^{10}Be and related ^{10}Be exposure ages for the southern Santa Catalina Mountains (Balco and others, 2008; http://hess.ess.washington.edu/math).

Naturally occurring beryllium typically is not found in significant quantities in quartz-bearing rocks that are not ore bearing. Contamination from cosmogenically produced ^{10}Be is possible, however, because the production rate in the atmosphere is higher than in rocks. ^{10}Be created in the atmosphere is transferred to the Earth's surface in rainfall and can be deposited in rocks along cracks or mineral boundaries. Therefore, ^{10}Be created in the atmosphere is a contaminant that must be removed from samples prior to analysis. Because ^{10}Be created in situ in quartz is the measurement goal, other mineralogic components of granites must be removed as well, including (but not limited to) micas and feldspars.

Sample Collection

We identified surfaces comprised of debris-flow deposits along the channels just downstream from Linda Vista, Pima, Finger Rock, Rattlesnake, and Soldier Canyons. These surfaces were on lands administered by the U.S. Forest Service and just upstream from private lands. Samples collected from Pima, Finger Rock, and Soldier Canyons were processed for cosmogenic ages; samples from the other drainages, and extra samples from the three principal drainages, were archived for potential later analyses. In addition to samples from these three canyons, we collected and analyzed samples from two extremely large boulders transported during the Ocho Grande debris flow, which occurred from an unnamed tributary at Tram Stop 8 in Sabino Canyon (Webb and others, 2008).

We collected samples from surfaces that were arranged vertically (stratigraphically) above the thalweg of the primary channels draining these canyons and had sufficient horizontal extent to be mappable. For example, see representative cross sections for Pima, Finger Rock and Soldier Canyons appear in Figure 11. For each surface, we selected a minimum of three boulders with the following characteristics: (1) the boulders had similar amounts of weathering and (or) desert varnish and appeared to be representative of primary deposition on the surface; (2) the boulders were stable and did not appear to have rolled following deposition; (3) the boulders had a relatively high amount of quartz with low feldspar and mica; (4) the top of the boulders either were at, or protruded above, the surrounding surface with minimal shielding from cosmic ray bombardment; and (5) the top of the boulders either were relatively level or had a measurable slope that would allow estimation of self shielding. Using a hammer and chisel, we collected 1.5 to 2.5 in. (3.75-6.25 cm) from the tops of these boulders. We collected 3-4 samples chiseled from boulders at each terrace level and also collected a whole boulder for possible future analysis.

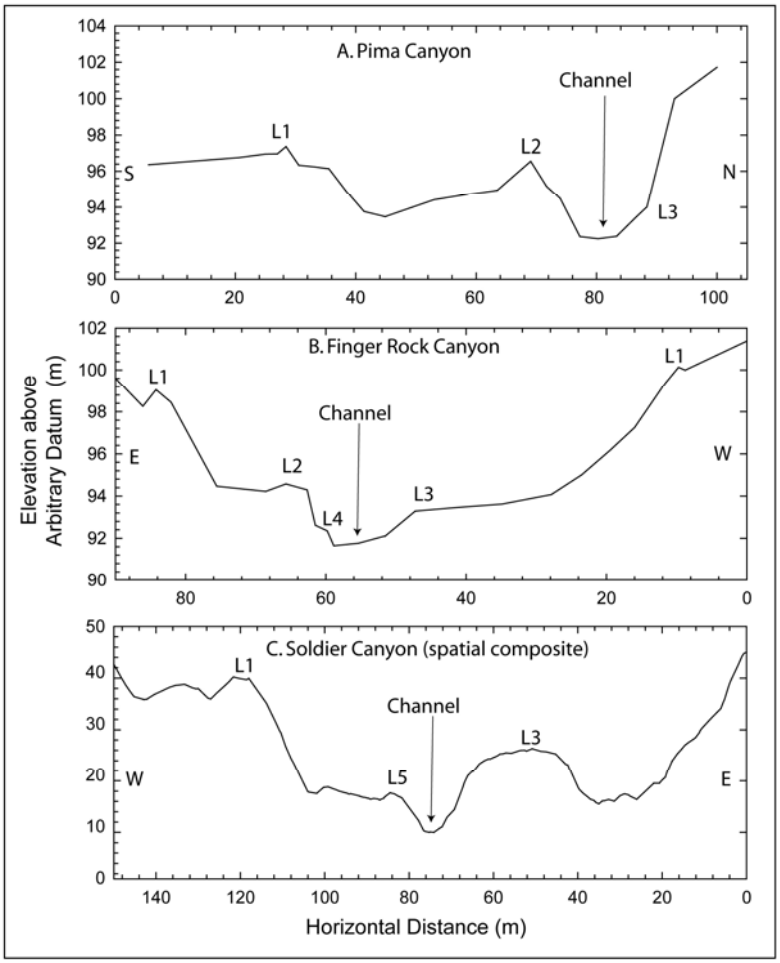

Figure 11. Cross-sections of levees sampled for cosmogenic dating from Pima Canyon (map DM-DF-1I), Finger Rock Canyon (map DM-DF-1G) and Soldier Canyon (map DM-DF-1B). Labels L1 – L5 are topographic positions associated with the sample numbers in Table 2. Refer to maps for ^{10}Be sample locations and ages, and to compare with relative geomorphic ages.

Sample Preparation

We selected three boulder samples from each site to analyze for ^{10}Be concentrations and to calculate exposure ages (see Table 2, Results Section). All of the samples we selected were chiseled pieces from the tops of boulders; no whole-rock samples were processed. We used a standard laboratory procedure to produce ^{10}Be targets for accelerator mass spectrometer analysis (Bookhagen, 2007) with some modifications as noted below.

Using a jaw crusher and a Biko grinder, we reduced the samples to sand-sized particles (< 2 mm) or finer diameter. We sieved the processed samples using disposable nylon sieves to obtain a particle fraction between 250 and 500 µm size for further analysis. Other size fractions were saved for potential future analyses, and in one case a saved fraction was processed. Our methods yielded a sample of 500 – 1000 grams (g) for extraction of cosmogenic ^{10}Be.

We used approximately 3L of 6N (1:1) HCl (hydrochloric acid) to soak the sample at 60º C for a minimum of 6 hrs (usually overnight) to remove fine particles, carbonates, and some Fe. After rinsing, drying, and

weighing of the remaining particles, on average 3% of the sample was removed at this step. We then used a 5% mixture of HF (hydrofluoric acid) and HNO_3 (nitric acid) to begin the process of etching quartz grains and dissolution of other minerals using a typical sample-to-liquid ratio of 30 grams/liter (g/L) and a temperature of 50-60º C for 8 hrs. Beginning with this step, all samples were held in HDE plastic containers to avoid boron (B) contamination, which is critical because the spectral emission signals of B and Be are overlapping; Pyrex glass (a borosilicate) is a common source of B contamination. Agitation was applied using a sonicator, which uses ultrasonic waves to induce particle motion and produce 55-60°C heat. The resulting loss of sample averaged 19% during this step. The remaining sample was put through a magnetic separator (Frantz) to remove any particles with magnetic properties, which typically included magnetite, apatite, and most of the micas; this step removed an additional 9% of the sample. Then the samples were further etched with a 1% HF/HNO_3 solution at a ratio of 15 g/L for 5-6 times in a sonicator or a hot-dog roller, which rotated and heated round plastic bottles bearing the samples and solutions. A sample was considered to be completed when a small aliquot yielded an Al concentration of <200 parts per million (ppm) from an ICP-OES (Inductively Coupled Plasma-Optical Emission Spectroscopy) mass spectrometer. This step ensures that most of the aluminum bearing minerals, such as feldspars and micas, are dissolved out of the sample during the etching steps. After all these steps, the average sample loss was 70%, resulting in samples that were 60-120 g and that visibly appeared to be quartz.

Approximately 30-40 g of each purified quartz sample were dissolved using concentrated HF acid. Accelerator mass spectrometers measure a ratio of $^{10}Be/^{9}Be$, and because ^{9}Be is present in quartz at extremely low concentrations, a carrier containing mostly ^{9}Be is added to the sample prior to total dissolution. For samples from debris-flow deposits thought to be of late Pleistocene age, this carrier was a standard beryllium solution (100 ppm Be, assumed to be all 9Be) with a $^{10}Be/^{9}Be$ of $1 . 10^{-14}$. For Holocene debris-flow samples, we created a custom carrier from the mineral phenacite (Be_2SiO_4), which yielded a solution of 220 ppm Be and a $^{10}Be/^{9}Be$ of $1 \cdot 10^{-16}$. To isolate beryllium – both cosmogenic ^{10}Be and carrier ^{9}Be – from other elements present in this purified quartz fraction, we totally dissolved the sample in concentrated HF at 60º C. By passing the sample through a cation-exchange column (to eliminate Fe and Na) followed by an anion-exchange column (to eliminate Al and Ti), the Be is extracted. Finally, elemental Be is converted to BeO_2 using a high-temperature furnace, mixed with elemental niobium (Nb), and packed into targets for accelerator analysis

Analysis of Targets

The ^{10}Be targets were analyzed using an accelerator mass spectrometer (AMS) designed to accurately measure this isotope at Lawrence Livermore National Laboratory in Livermore, California (https://cams.llnl.gov/). This AMS is the most appropriate one in the United States for Holocene ages because it has a ratio resolution of $^{10}Be/^{9}Be$ of $1 \cdot 10^{-16}$, which is required to obtain measurements on the minute quantities of ^{10}Be that would be present in 1,000-year-old deposits. To gain higher beam strengths from targets, this laboratory switched from silver (Ag) to niobium (Nb), which increases the yield in the spectral widths for beryllium and increases the accuracy of measurements. The results are a ratio of $^{10}Be/^{9}Be$ that must be converted to the number of atoms per gram of sample.

Bookhagen (2007) provides the framework for calculations of ^{10}Be ages from $^{10}Be/^{9}Be$ ratios, and the process essentially is as follows: (1) knowing the precise mass of quartz in the sample, as well as the mass and concentration of the carrier, one can calculate the number of atoms of ^{9}Be per gram that were present in the sample after carrier addition; it is assumed that the 9Be added to the dissolved quartz is much greater than any naturally occurring ^{9}Be in the quartz itself; (2) given the $^{10}Be/^{9}Be$ ratio, the

atoms/g of ^{10}Be can be calculated; (3) the latitude, longitude, and elevation of the sample location are known to allow for production-rate variation across the planet; (4) any local shielding corrections need to be estimated (1 = no shielding, 0 = totally shielded); and (5) the thickness of the sample that was collected. These input values are presented in their entirety as Appendix 1 of Webb and others (2008). Once these quantities are known, the CRONUS-Earth calculator (http://hess.ess.washington.edu/math) can be used to estimate ages of samples.

RESULTS

GIS-Derived Basin And Stream Characteristics

Basin and channel morphometric parameters were derived for each study canyon, and also for Rattlesnake Canyon, a tributary to Sabino Wash (Table 1). Stream profiles were developed from channel gradients derived from 10-m DEMs and are plotted according to basin size for easier comparison (Figures 12-14). Stream profiles are plotted such that zero channel length (right side of x-axis) approximately corresponds to where the stream exits the mountain front.

Table 1. Basin and channel morphometrics.

Canyon Name	Basin Orien-tation	Area (mi^2)	Area (km^2)	Basin Length (mi)	Basin Length (m)	Ave Basin Slope (°)	Melton Ratio	Relief Ratio	Ave Channel Grad (%)
Agua Caliente	SW	12.7	33.0	5.0	8,079	18	0.19	0.14	6
La Milagrosa	SW	4.7	12.1	4.3	6,915	23	0.26	0.13	7
Molino*	SW	6.7	17.4	5.7	9,161	26	0.31	0.14	10
Soldier*	SW	3.9	10.0	4.4	7,134	24	0.33	0.15	11
Gibbon*	SW	1.2	3.1	2.6	4,145	26	0.49	0.21	16
Bear*	SW	16.8	43.6	8.5	13,662	26	0.27	0.13	7
Sabino*	S	35.2	91.3	8.4	13,457	27	0.21	0.15	7
Bird*	S-SW	2.3	6.0	3.1	4,927	31	0.46	0.23	15
Esperero*	S	3.5	8.9	3.5	5,598	31	0.49	0.26	16
Ventana*	S-SE	3.8	9.9	3.2	5,136	32	0.41	0.25	14
Pontatoc	W-SW	1.7	4.4	2.6	4,186	30	0.55	0.27	19
Finger Rock	SW	1.6	4.2	2.8	4,461	34	0.62	0.28	20
Cobblestone	SW	0.8	2.0	1.5	2,355	33	0.62	0.37	19
Pima	W-SW	4.2	10.9	3.7	6,016	33	0.39	0.21	13
Pusch	SW	0.5	1.3	1.2	1,871	31	0.63	0.38	23
Linda Vista	NW	0.3	0.8	1.0	1,617	30	0.87	0.50	23
Rattlesnake[#]	S	2.3	6.0	2.9	4,676	29	0.49	0.25	13

*Canyons with debris flows in 2006 (Webb and others, 2008).

[#] Rattlesnake Canyon was not mapped as part of this study. In 2006, debris flows from Rattlesnake Canyon flowed into Sabino Canyon.

A direct comparison of study canyon morphometrics with reported data describing debris-flow prone basins is difficult, as reported data are either from regions with very different climates (Wilford and others, 2004) or from highly disturbed basins (Cannon and Gartner, 2005). In addition, all of the study canyons have evidence of past debris-flow activity. These data are more useful for assessing the influence of basin size and channel gradient on debris-flow conveyance and potential runout distances. A review of Table 1 shows that the largest basins also have the lowest channel gradients: Aqua Caliente, La Miligrosa, Molino, Bear and Sabino Canyons. Three of these canyons – Molino, Bear, and Sabino – had debris flows in 2006 (Webb and others, 2008). Debris flows in these canyons formed on steep sideslopes, flowed into the main channel and either terminated at the channel junction or traveled a short distance downstream before depositing.

In contrast, six smaller, steeper basins with debris flows in 2006 behaved differently. These canyons include Soldier, Gibbon, Bird, Esperero, Ventana, and Rattlesnake Canyons. Debris flows in Esperero and Ventana Canyons were limited to the upper watersheds (Webb and others, 2008), while debris flows in Soldier, Gibbon, Bird and Rattlesnake exited or almost exited the mountain front. In Rattlesnake Canyon slope failures coalesced into a debris flow which traveled 2.4 miles downstream into Sabino Canyon where 15 -20 feet of sediment was then deposited (Webb and others, 2008). Debris flows in both Gibbon and Soldier Canyons exited the mountain front and deposited in developed areas. Debris flows in Bird Canyon also exited the mountain front but were confined within a deeply incised channel. Basin responses to the 2006 rainfall indicates that smaller, steeper basins have a greater potential for exiting the mountain front than those generated in larger basins with lower-gradient channels.

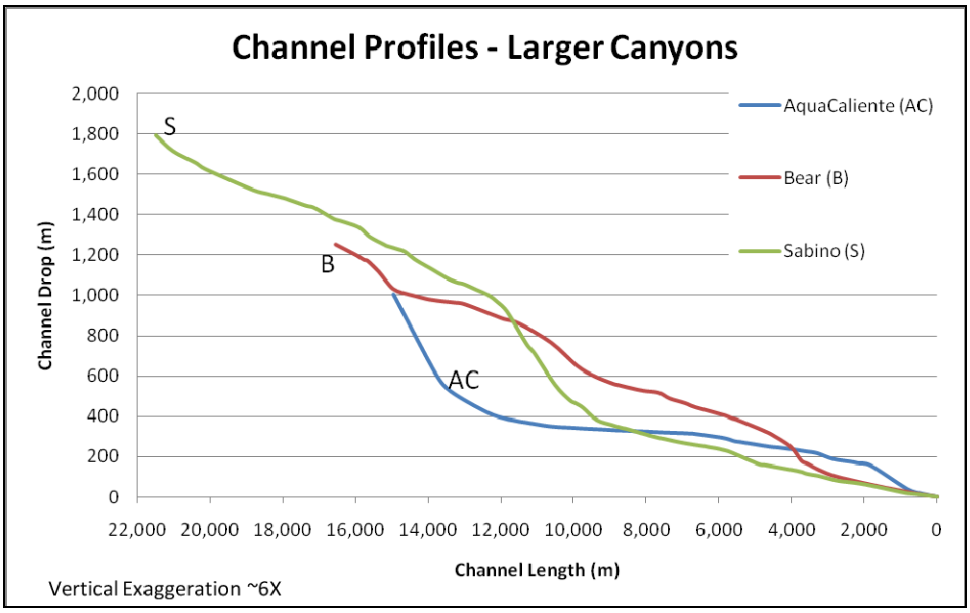

Figure 12. Stream profile plots of the three largest study basins. Bear and Sabino Canyons has debris flows in 2006. Sabino and Bear Canyons had debris flows in 2006.

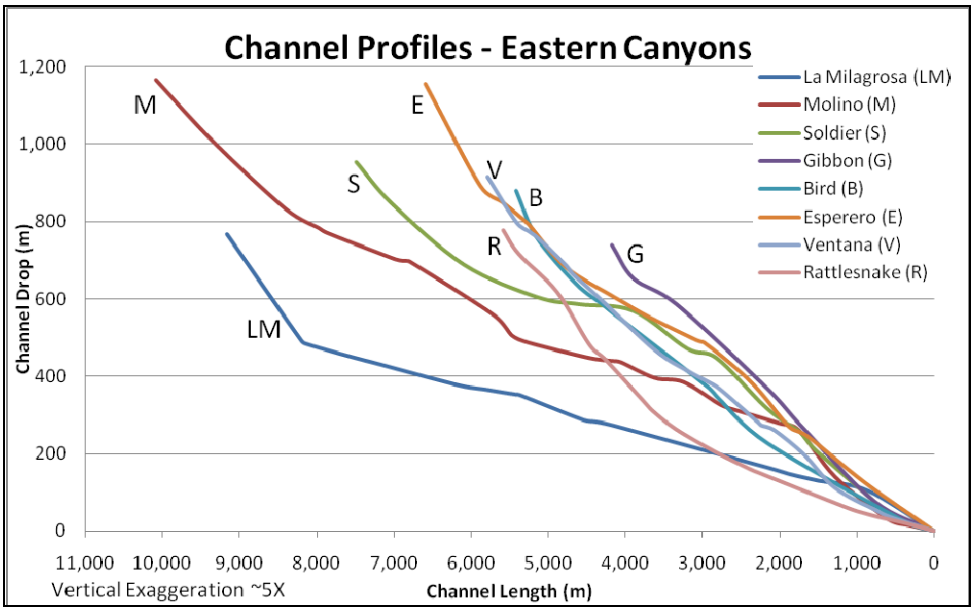

Figure 13. Stream profile plots of the eastern study basins. Note stream channel length compared to plots in figures 12 and 14. Soldier, Gibbon, Rattlesnake, Bird, and Esperero Canyons had debris flows in 2006. Rattlesnake Canyon was not included in the mapping.

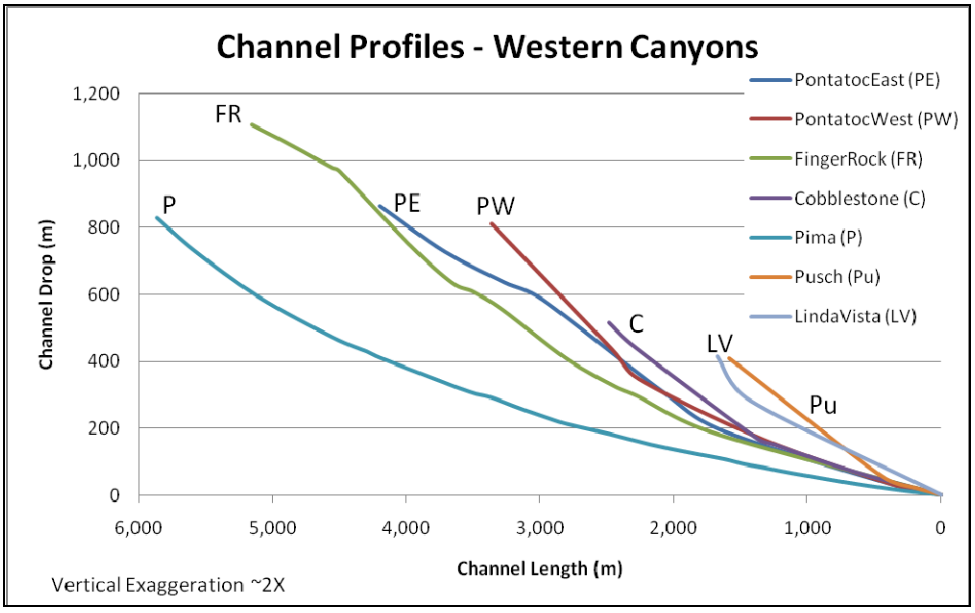

Figure 14. Stream profile plots for the western study basins. Note channel lengths compared to eastern channels.

Geologic Mapping

Agua Caliente-La Milagrosa-Molino Canyons

The drainages of Agua Caliente, La Milagrosa, and Molino Canyons (Figure 1, map DM-DF-1A) begin as steep, bedrock lined, incised channels that eventually widen into sandy washes and merge further downstream to form Agua Caliente Wash. Below the confluence of these three washes, the channel floor is alternately lined by coarse sandy deposits and large boulders. The sandy channel sections are dynamic and change with each significant flow. Boulder deposits within the active channel are exhumed or buried on a regular basis. Coarse cobble and boulder deposits lining channel walls extend approximately 1 mile (mi, 1.5 km) downstream from the confluence. Debris-flow deposits in Agua Caliente, La Milagrosa, and Molino Canyons are preserved on bedrock ledges, adjacent to bedrock channel walls, flanking active channels, and as levees or terraces inset into existing debris-flow deposits.

Pleistocene debris-flow deposits (unit I) are exposed in channel bottoms, within the walls of incised drainages, and on steep rocky shelves in bedrock-lined stretches of canyons. These deposits are typically overlain by younger debris-flow deposits and fine-grained Holocene alluvium. Older debris-flow deposits (units YI1 and YI2) deposits are the highest debris-flow deposits in the mapped area. Unit YI1 stand up to 12 ft (3.5 m) above the active channel. Where deposited adjacent to bedrock, YI1 deposits are generally narrow (less than 5 m across) open-framework boulder levees with little or no fine matrix sediment preserved. YI1 deposits are more widespread downstream and are typically covered by fine grained sediment (likely derived from both fluvial and eolian sources) and dense vegetation. Large cobbles and boulders are exposed in the steep, near vertical flanks of these deposits. YI2 deposits stand 6-10 ft (2-3 m) higher than the active channel and are usually inset into YI1 deposits. YI2 deposits form long stretches of the modern channel wall in Molino Canyon and consist of clast-supported cobble and boulder deposits deposited adjacent to exposed bedrock walls.

Early to late Holocene debris-flow deposits (units Y1, Y2, and Y3) are found nearer to, and are less elevated (within 5 ft [1.5 m]) relative to, the active channel. Intermediate debris-flow deposits (unit Y1) are typically inset below adjacent older debris-flow deposits, and generally do not include boulders greater than 3 ft (1 m) in diameter. The few large boulders encountered in inset Y1 deposits may be derived from older, higher-standing YI2 and YI1 deposits. Young debris-flow deposits (unit Y2) are generally found within 3 ft (1 m) of the active channel and are of limited extent within the canyons probably due to the confined, highly active, erosive channel and near channel environment. Where preserved, Y2 deposits are observed as large cobble to medium boulder lobes near channel walls. Y2 deposits are locally covered by sand bars deposited by recent flows and often exhibit polished boulder faces from stream abrasion. Very young debris-flow deposits (unit Y3) range in size from cobbles to medium boulders and generally lack vegetation due to frequent inundation and lack of soil development. Sandy channel sediments mantle significant portions of Y3 deposits resulting in polished boulder faces. The exposed extent of Y3 deposits likely changes with each significant flow, as pool and riffle sequences alternately bury and exhume Y3 deposits. Bouldery stretches of the active channel are sometimes difficult to discern from flanking Y3 deposits. These rocky reaches may be highly eroded or reworked Y3 and higher debris-flow deposits.

Elongate cobble- and boulder-dominated deposits (unit B) flank both sides of Agua Caliente Wash downstream from the confluence of Agua Caliente, La Milagrosa, and Molino Canyons. These deposits resemble debris-flow levees but may also be cobble and boulder deposits reworked by fluvial processes. Fine sediments of B deposits located near the active channel have been removed by fluvial reworking. B

deposits located above the active channel are commonly buried by fine sediments either from initial deposition and subsequent abandonment, soil accumulation, or overbank deposition. Coarse cobble- and boulder-dominated deposits derived from reworked debris-flow deposits (unit C) are found in channel bottoms or forming channel banks. These deposits generally do not exhibit sorting when viewed in channel banks, but also do not exhibit defining debris-flow deposit characteristics. Unit C deposits have probably been winnowed and reworked by fluvial processes.

Soldier Canyon

Soldier Canyon (Figure 1, map DM-DF-1B) is drained by Soldier Wash, which flows under the Catalina Highway through two 6 ft (2 m) box culverts and continues downstream to exit the mountain front near the Mount Lemmon Short Road, approximately ½ mile (1 km) below the box culverts. Pleistocene debris-flow deposits (unit I) were observed along Soldier Wash above and below the Mount Lemmon Highway at the box culverts. In Soldier Canyon, these are the highest standing debris-flow deposits, forming terraces up to 16 ft (5 m) above the active channel. Older Holocene to latest Pleistocene debris-flow deposits (unit YI) are inset 3-7 ft (1-2 m) below I deposits. On the Soldier Canyon fan, downstream of the Mount Lemmon Short Road, YI deposits are farthest removed from the active channel area.

Intermediate debris-flow deposits (unit Y1) are generally found 3 to 10 ft (1-3 m) above the active channel near the mountain front. On the Soldier fan they define the lateral extent of recent channel migration. Young debris-flow deposits (unit Y2) are generally found less than 3-5 ft (1-1.5 m) above the active channel and are inset below Y1 deposits. Very young debris-flow deposits (unit Y3) are found within or adjacent to the active channel upstream of the fan apex. Coarse boulder bars of uncertain origin (unit B) were mapped farther out on the fan, near Snyder Road. These deposits probably represent reworked debris-flow deposits. Unit B deposits were used to define the general downstream extent of debris flows on the Soldier fan.

During mapping we observed an open septic-system test pit, approximately 6 ft (2 m) deep, on a late Pleistocene to early Holocene alluvial fan surface. The fan surface was smooth and fine-grained with no observable evidence of debris-flow deposits. The upper 2 ft (0.5 m) of the pit was composed of sand, silt and fine gravel, presumably deposited by sheetflooding on the fan. The bottom 5 ft (1.5 m) was entirely composed of unsorted boulders likely derived from debris flows (Figure 15). This exposure demonstrates that subsequent burial has obscured some older debris-flow deposits. While YI debris-flow deposits are not mapped very far south of the Mount Lemmon Short Road, it is likely they are present below the surface.

Soldier Canyon was heavily impacted by the July 2006 storms. Webb and others (2008) documented 56 hillslope failures within the Soldier Canyon watershed. These hillslope failure coalesced into debris flows that travelled down canyon, under and over the Catalina Highway, and down Soldier Wash. Comparisons of orthophotographs taken in 2002 and 2007 show significant channel widening and alluvial deposition resulting from the 2006 debris flows and floods (Figure 16). Sediment from at least two debris-flow pulses were deposited on the Soldier fan (Figure 17).

Figure 15. Septic system test pit on Soldier fan. Note smooth fan surface. Upper portion of the pit is finer-grained sediment while the bottom 1.5 m is composed of boulder debris-flow deposits.

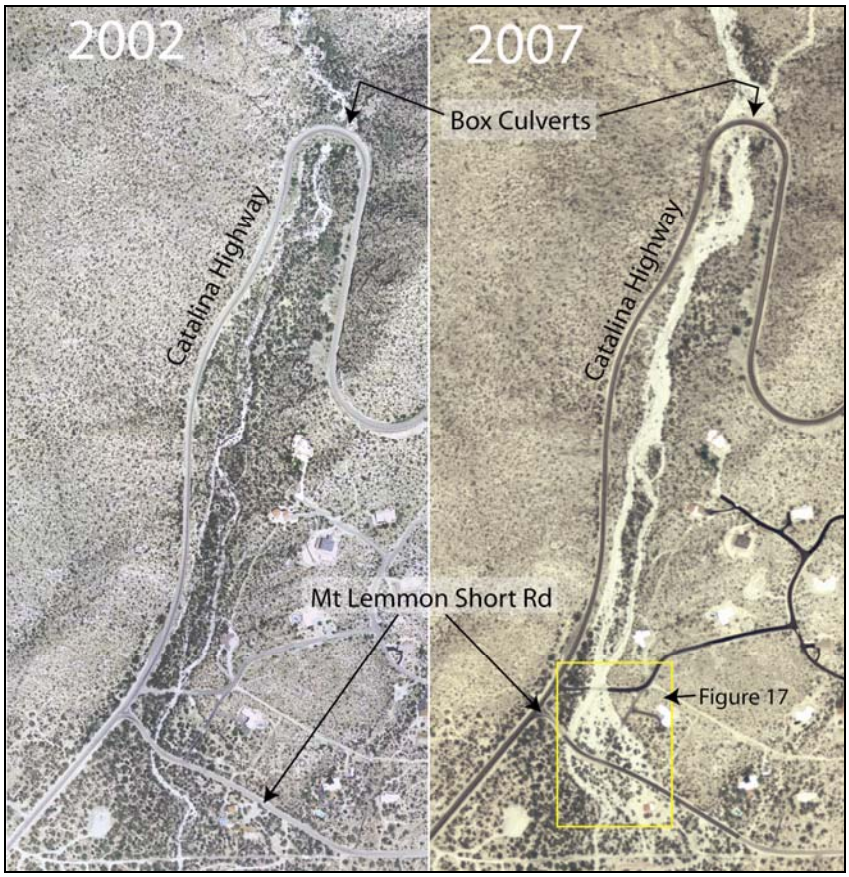

Figure 16. Comparison of Soldier Wash channel between 2002 (left) and 2007 (right). Debris flows and floods significantly widened the channel; older, abandoned channels were re-occupied. Yellow box shows area in Figure 17.

Our mapping efforts originally focused only on prehistoric debris-flow deposits. Late in 2007 the scope of work was expanded to include mapping debris-flow deposits from 2006 in Soldier Canyon. By the time this decision was made significant changes to the channel on the fan had occurred through subsequent rainfall runoff events and by heavy equipment reforming and opening the channel to allow

flow under the bridge. Therefore, most of the debris-flow deposits in the vicinity of the Mount Lemmon Short Road were mapped using a combination of aerial and ground photographs taken by the USGS and the AZGS in August and September of 2006, and by extensive field observations made throughout 2007. Other 2006 debris-flow deposits above the Soldier fan were more persistent and thus were mapped in the field (Figure 17, map DM-DF-1B). Based on these data there were at least two debris-flows that traveled to the Mount Lemmon Short Road (Figure 17). The first pulse apparently plugged the bridge. The second pulse stopped and deposited a boulder snout just upstream of the bridge and on top of the first pulse (Figures 8 and 17). These two pulses likely forced recessional flood flow eastward (Figures 16 and 17).

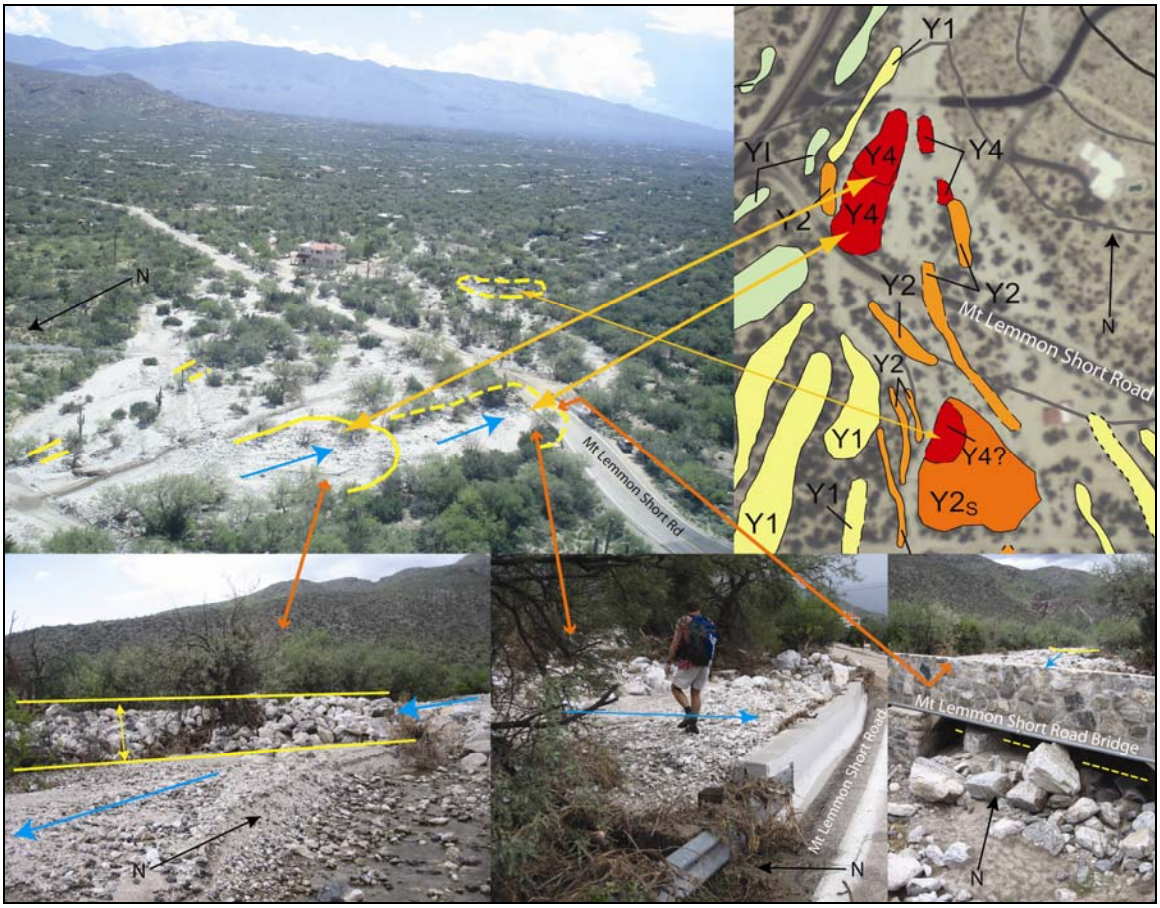

Figure 17. Soldier Fan debris-flow deposits, 2006. Upper left: oblique view to southeast showing debris-flow deposits (Y4) at and above Mt Lemmon Short Road, and a potential debris-flow deposit (Y4?) below the road (P.G. Griffiths, Sept. 13, 2006). Upper right: clip of map DM-DF-1B showing locations of Y4 deposits. Lower left (same as Figure 8): view northwest of Y4 deposit above Mt Lemmon Short Road (P.G. Griffiths, Sept. 12, 2006). Lower middle: view east of Y4 deposit at Mt Lemmon Short Road bridge (C.S. Magirl, Sept 12, 2006). Lower right: view north of two Y4 debris-flow deposits at and above Mt Lemmon Short Road (P.A. Pearthree, Aug. 6, 2006). See text for discussion.

Two other very small debris-flow deposits are mapped in the area above the Mount Lemmon Short Road (Figure 17). These may be from small debris flows or remnants of larger debris flows that were later reworked. Downstream of the Mt. Lemmon Short Road two possible 2006 debris-flow deposits are labeled “Y4?”. These are relatively coarse, poorly sorted deposits that have debris-flow characteristics, but it is possible they were reworked by flooding associated with the 2006 events. They may be debris-

flow deposits, re-worked debris-flow deposits, or flood-related deposits. These 2006 deposits (unit Y4?) were emplaced in boulder zones of older debris-flow deposits (Unit Y2) visible on the 1960 aerial photographs.

Gibbon Canyon

Gibbon Canyon Figure 1, map DM-DF-1C) is an informally named canyon with a small, steep, bedrock-incised channel. Downstream from the mountain front the channel remains entrenched within older alluvial deposits. Deposits generally fine downstream, although coarse boulder deposits have been intermittently emplaced within the alluvial sediments. The finer grained, sandy fluvial channel sediments are continually reworked and change with each significant flow. Boulder deposits within the active channel are exhumed or buried on a regular basis. Coarse cobble and boulder deposits lining channel walls extend approximately 0.5 mi (1 km) downstream from the mountain front. In-channel boulder deposits extend much further, and are probably fluvially reworked. Debris-flow deposits in Gibbon Canyon are preserved on bedrock ledges, adjacent to bedrock walls, flanking active channels, in channels as snouts or levees, or on terraces inset into older debris-flow deposits.

Latest Pleistocene to early Holocene deposits (units YI1 and YI2) are the highest standing debris-flow deposits in Gibbon Canyon. Younger debris-flow deposits are commonly inset into unit YI1 and YI2. Unit YI1 stands up to 16 ft (5 m) above the active channel near the mountain front. Some YI1 levees are long continuous deposits (up to 250 ft [75 m]) and are more than 23 ft (7 m) across. Fine-grained matrix sediments have been entirely removed from the exposed part of these deposits. More widespread YI1 deposits are typically covered by fine-grained sediment, likely derived from both fluvial and eolian sources, and dense vegetation including mature mesquite, acacia, prickly pear, cholla, barrel cactus, and numerous tall grasses and shrubs. Large cobbles and boulders are exposed in the steep, near vertical flanks of these deposits. YI2 deposits stand less than 13 ft (4 m) above the active channel and are often adjacent to YI1 deposits. YI2 deposits form long stretches of the modern channel walls, ranging up to 650 ft (200 m) in length. In this setting, YI2 deposits form relatively planar ledges with moderately rounded edges and near vertical exposures of clast-supported cobble and boulder deposits in channel walls. In the upper reaches of Gibbon Canyon, YI1 and YI2 deposits are well-preserved, prominent features on the landscape.

Early to late Holocene deposits (units Y1, Y2, and Y3) are less than 10 ft (3 m) above the active channel. In the upper reaches of the map area, intermediate debris-flow levees (unit Y1) are part of the prominent suite of terraces, along with the YI units. Young debris-flow deposits (unit Y2) are generally found less than 7 ft (2 m) above the active channel and are of limited extent probably due to their close proximity to the active channel. Fine-grained matrix sediments are typically absent from Y2 deposits, leaving only large cobble to medium boulder lobes near channel walls. Y2 deposits are occasionally covered by sandy bars deposited by recent channel flows and often exhibit polished boulder faces from stream abrasion. Very young debris-flow deposits (unit Y3) are composed of cobbles to boulders deposited as prominent snouts and levees within or immediately adjacent to the active channel. Vegetation is typically absent from Y3 deposits due to frequent flood inundation and lack of soil development. Sandy channel sediments mantle significant portions of Y3 deposits. The exposed extent of Y3 deposits likely changes with each significant flow. Bouldery stretches of the active channel are difficult to discern from flanking Y3 deposits.

The focus of this mapping effort was on prehistoric debris-flow deposits. Debris-flow deposits from 2006 were not specifically mapped in Gibbon Canyon, although the downstream extent of these deposits are

shown with a red hatched line on map DM-DF-1C. The 2006 debris-flow terminus lies at the end of the bedrock reach of the canyon. There was no evidence to suggest that the debris flows had progressed through the culvert underneath North Mesquite Canyon Place road. Downstream from that point, there was significant aggradation by fluvial sediments. Based on geomorphic and biotic evidence (e.g. no significant impacts on vegetation), there was no apparent debris-flow activity downstream of the bedrock canyon exit. However, it should be noted that numerous, very young (Y3) debris flow levees *or* fluvially deposited boulder trains and splays extend up to 0.5 mi (0.8 km) downstream from the extent of 2006 debris flows. Furthermore, there are numerous boulder deposits that are likely remobilized boulders by extreme discharge floods.

Sabino and Bear Canyons

Sabino and Bear Canyons (Figure 1, map DM-DF-1D) have bedrock-incised channels incised to the mountain front where channels become entrenched in older alluvial deposits. Boulder deposits within the active channel are reworked and exhumed or buried on a regular basis. Coarse cobble and boulder deposits lining channel walls extend approximately 1.2 miles (2 km) downstream from the mountain front. In-channel boulder deposits extend much further and have been reworked by floods. Below the confluence of Bear and Sabino Creeks, exposed debris-flow levees and snouts diminish rapidly. However, there is much evidence for significant fluvial deposition downstream of the mountain front, so there are likely numerous buried debris-flow deposits. In general, Sabino Canyon does not have many exposed debris-flow deposits in the mapped area. This lack of debris flows may be due to the consistent fluvial burial of coarse-grain sediments, and storage of more recent debris-flow deposits in the canyon upstream. Sabino and Bear Canyons are the largest of the study canyons. Both canyons have basin-average channel gradients of 7% (Table 1), although near the mountain front channel gradients in both canyons reduce to approximately 3% (Figure 12). This lower channel gradient significantly reduces channel sediment-carrying capacity, thus debris flows in these canyons probably do not exit the mountain front as frequently as basins with steeper channels. Indeed, in 2006 numerous debris flows occurred in lower Sabino and Bear Canyons, yet all flows terminated at the mainstem channel and did not exit the mountain front into the mapped areas.

Late Pleistocene debris-flow deposits (unit I) are exposed on the tops of some terraces. Locally, unit I deposits are overlain and partially buried by fine-grained Holocene alluvium, reducing the local microtopography. Few Pleistocene deposits remain exposed; most have been buried by fluvial activity. Older debris-flow deposits (unit YI, YI1,and YI2) have similar characteristics. YI1 and YI2 are delineated near the mountain front, and undifferentiated farther out. YI deposits tend to define the Holocene channel, providing a barrier for flooding. Some YI1 deposits are up to 1640 ft (500 m) long, and less than 23 ft (7 m) wide. YI1 deposits are the highest standing debris-flow deposits along the channel margins, up to 13 ft (4 m) above the active channel. Younger debris-flow deposits are commonly inset into YI1 deposits. YI1 deposits are often covered by fine-grained sediment (likely derived from both fluvial and eolian sources). In the upper reaches of the map area, YI1 deposits are well-preserved, prominent features on the landscape. YI2 deposits stand 3-10 ft (1-3 m) above the active channel and are often adjacent to YI1 deposits. YI2 deposits form long stretches of the modern channel walls, ranging up to 1000 ft (300 m) in length, and less than 20 ft (6 m) wide. YI2 deposits are relatively well preserved above the channel confluence of Sabino and Bear Canyons, and are prominent features on the landscape.

Early to late Holocene units (units Y1, Y2 and Y3) stand 3-10 ft (1-3 m) above the active channel. Intermediate debris-flow deposits (unit Y1) are often part of the suite of terraces rising above the active channel. Young debris-flow deposits (unit Y2) are generally found within 7 ft (2 m) of the active channel

and are of limited extent. Very young debris-flow deposits (unit Y3) are composed of cobbles to boulders deposited within or adjacent to the active channel. Vegetation is typically absent from Y3 deposits due to frequent flood inundation and lack of soil development. Sandy channel sediments often mantle significant portions of Y3 deposits resulting in polished boulder faces. The exposed extent of Y3 deposits likely changes with each significant flow. Bouldery stretches of the active channel may be Y3 deposits, or they may be reworked older deposits. At Sabino and Bear Canyons, the most prominent snouts are Y3 deposits.

Elongate cobble and boulder-dominated deposits (unit B) lie downstream of the confluence of Sabino and Bear canyons, in Sabino Creek. B deposits resemble debris-flow levees but are likely just reworked fluvial (flood) deposits. The presence of unit B deposits were used to define the downstream extent of debris-flow deposits.

Bear Canyon, Sabino Canyon and Rattlesnake Canyon, a tributary to Sabino Canyon, had debris flows in 2006 (Webb and others, 2008), however none of the debris flows extended into the mapped area. Numerous 2006 debris flows occurred in lower Sabino and Bear Canyons; most of these terminated at the mainstem channel and did not travel significant distances downstream (Webb and others, 2008). The debris flows from Rattlesnake Canyon flowed into Sabino Canyon and traveled down-channel for a short distance before deposition (Webb and others, 2008).

Esperero and Bird Canyon

Esperero and Bird Canyons (Figure 1, map DM-DF-1E) are narrow bedrock-confined channels that are deeply entrenched and have extremely coarse-grained channel deposits. The drainages are narrow and choked with large boulders and numerous debris-flow deposits. The active channels within the canyon walls are extremely rocky and narrow, rarely exceeding 16 ft (5 m) width. As the channels exit the canyons, they remains deeply entrenched (13-20 ft [4-6 m] in Esperero Canyon; 10-13 ft [3-4 m] in Bird Canyon) and very narrow. Based on the local topography and channel -banks exposures of very coarse, poorly to non-sorted sediment, the alluvial fans near the mountain front have likely been constructed mainly by debris-flow activity.

Pleistocene deposits (unit I) are exposed on the tops of terraces within 0.6 miles (1 km) downstream of the mountain front. Unit I deposits have been overlain and buried by fine-grained Holocene alluvium which has limited their surface exposure. Older debris-flow deposits (units YI, YI1 and YI2) are similar. YI1 and YI2 are delineated in the upper reaches of Esperero Canyon where inset relationships can be seen. In the lower reaches of Esperero Canyon, YI units cannot be differentiated. YI1 deposits are especially high-standing debris-flow deposits, up to 20 ft (6 m) above the active channel and are often inset with younger debris-flow deposits. Some YI1 levees exhibit lengths of 650 ft (200 m), and widths of approximately 16 ft (5 m). Two prominent YI snouts coalesce to the east side of the main channel in Esperero Canyon (YI1), and to the west of the main channel in Bird Canyon (YI2), immediately downstream of the canyon mouths. YI2 deposits stand 10-13 ft (3-4 m) above the active channel and are usually adjacent to YI1 levee deposits. Overall, YI2 deposits are very similar in appearance to YI1, however their lower landscape position is adequate to place them as their own unit. Some YI2 levees exhibit lengths of 1000 ft (300 m), and widths of only 16 ft (5 m).

Intermediate debris-flow deposits (unit Y1) are generally found 7-10 ft (2-3 m) above the active channel, and are typically inset into older debris-flow deposits. These deposits tend to lie at the base of slopes and act as channel-confining levees. Young debris-flow deposits (unit Y2) are generally found 3-7 ft (1-2

m) above the active channel. Exposure of very young debris-flow deposits (unit Y3) appears to be dynamic, changing with significant flows due to continual exhumation and burial. Some Y3 deposits may be reworked older deposits. A prominent Y3 snout is mapped south of East Sunrise Drive. Elongate boulder deposits (unit B) lie in Esperero Canyon downstream of the confluence with Bird Canyon. These resemble debris-flow levees but are likely reworked fluvial (flood) deposits.

The focus of this mapping effort was on prehistoric debris-flow deposits. Debris-flow deposits from 2006 were not specifically mapped although the downstream extent of these deposits are shown with a red hatched line on map DM-DF-1E. Both Esperero and Bird Canyons had debris-flow activity in 2006. Debris flows in Esperero Canyon were limited to the upper basin and did not extend into the mapped area (Webb and others, 2008). The extent of 2006 debris-flow deposits in Bird Canyon is located just upstream of the confluence with Esperero Canyon. There was no field evidence of debris flows from 2006 downstream of the confluence, although significant amounts of water-lain sediment were deposited downstream. This determination of downstream extent is based on field, geomorphic evidence. It is possible that a minimal volume of the debris flows entered Esperero Canyon from Bird Canyon, but subsequent flooding eroded any evidence.

Ventana Canyon

Ventana Canyon (Figure 1, map DM-DF-1F) is a narrow bedrock canyon, with a deeply entrenched channel and extremely coarse-grained channel material. The drainage is narrow and choked with large boulders and numerous debris-flow deposits. The active channel within the canyon walls is extremely rocky and narrow, rarely exceeding 16 ft (5 m) across. As the channel exits the canyon, it remains very narrow and is entrenched 6-10 ft (2-3 m) below adjacent alluvial fan surfaces. The original active channel that drains Ventana Canyon has been highly altered by residential and commercial development, making identification of debris-flow deposits very challenging. Based on local topography and channel-bank exposures of the underlying sediment, the Ventana Canyon alluvial fan complex was constructed mainly by debris-flow activity. At the canyon mouth, debris-flow levees on the alluvial fan splay considerably; the total width of the young debris-flow deposits widens to 1150 ft (350 m).

Latest Pleistocene to early Holocene units YI1 and YI2 are delineated in the upper reaches of Ventana Canyon where inset relationships can be seen. In the lower reaches of Ventana Canyon, YI units cannot be differentiated. YI1 deposits are high-standing debris-flow deposits, up to 16 ft (4 m) above the active channel and are commonly inset by younger debris-flow deposits. Some YI1 levees exhibit lengths of 330 ft (100 m), and widths of only 16 ft (5 m). A prominent YI1 snout lies to the east side of the main channel, immediately downstream of the canyon mouth. YI2 deposits stand 10-13 ft (3-4 m) above the active channel and are adjacent to YI1 levee deposits. Overall, YI2 deposits are very similar in appearance to YI1, however their landscape position and inset relationships are adequate to place them as their own unit. Some YI2 levees exhibit lengths of 1000 ft (300 m), and widths of only 16 ft (5 m).

Intermediate debris-flow deposits (unit Y1) are generally 3-10 ft (1-3 m) above the active channel and tend to lie at the base of slopes, acting as channel-confining levees. Young debris-flow deposits (unit Y2) are generally found above the active channel 3-7 ft (1-2 m) and Y3 deposits are within or adjacent to the active channel. Very young debris-flow deposits (unit Y3) are subjected to reworking and erosion due to their proximal location to the active channel. The exposed extent of Y3 deposits changes with significant flows. Some Y3 deposits may include older debris-flow deposits.

Finger Rock and Pontatoc Canyons

Finger Rock and Pontatoc Canyons (Figure 1, map DM-DF-1G) have narrow, bedrock-confined channels within the canyons that remain entrenched within older alluvial deposit at below the canyons mouths. Finger Rock Wash exits the mountain front approximately ½ mile (1 km) upstream from the confluence with Pontatoc Wash. The upper portion of Finger Rock fan is on national forest land so debris-flow deposits have been well-preserved. Pontatoc Wash exits the mountain front at the national forest boundary where it joins with Finger Rock Wash. Outside of the national forest, Finger Rock fan has been heavily developed thus most evidence of on-fan older debris-flow deposits (unit YI) are obscured. In addition, the channel of Finger Rock Wash has been highly disturbed as the floodplain is used as a utility corridor.

Due to the amount of residential development on the Finger Rock fan, mapping of debris-flow deposits on the fan surface required extensive use of the 1960 aerial photographs. These photos show numerous, large debris-flow deposits with very large clasts on top of the fan along Finger Wash and at the mouth of Pontatoc Wash. Some remnants of these deposits can still be seen between houses, and along many foundations on Finger Rock fan. Also visible in the photos are old channels plugged by debris-flow deposits. Based on these photos, it appears that Pontatoc Wash and Finger Rock previously drained in a more westerly-southwesterly direction in the latest Pleistocene to early Holocene. As sediment from large debris flows (unit YI) plugged channels, subsequent flows were forced southward into the modern channel.

Finger Rock and Pontatoc Washes are incised up to 25 ft (8 m) below adjacent fan surfaces. Development along these washes has occurred on geologic floodplains within 3-10 ft (1-3 m) above active channels. Mapping within the recent floodplain relied heavily on 1960 aerial photographs. The modern channel and geologic floodplain flow south-southeast and are confined to a 10-25 ft (3-8 m) deep corridor between Pleistocene fan deposits and/or Tertiary Pantano Formation (Klawon and others, 1999). Older boulder deposits (unit YI) were found surprising far downstream, approximately 2 channel miles (3km) from the Finger Rock fan apex. As with Esperero and Pima Canyons, confinement of the geologically active floodplain was necessary for debris flows to travel so far downstream. These deposits were most likely not emplaced by one debris flow, but rather by multiple debris flows or large floods, which broke through previous debris-flow deposits and re-initiated traveled downstream. Debris-flow deposits found so far from the mountain front exhibit characteristics of older YI deposits. It is unlikely debris flows in this channel could travel such distances with modern conditions within this wash.

Pleistocene debris-flow deposits (unit I) were observed along Finger Rock Wash above the Coronado National Forest boundary. Older debris-flow deposits (units YI1 and YI2) are the highest standing debris-flow deposits in both Finger Rock and Pontatoc Canyons. In Finger Rock Canyon unit YI deposits are against unit I deposits. Two different levels of YI deposits can be identified in these canyons and on the fan surface. The relationship between YI1 and YI2 deposits is lost mid-fan, approximately 1.5 channel miles (2.5 km) downstream from the fan apex. The two levels of YI provide information about channel migration across the fan surface before entrenchment of the modern channel.

Intermediate debris-flow deposits (unit Y1) are generally found less than 7-13 ft (2-4 m) above the active channel near the mountain front. Farther downstream Y1 deposits may be 3-7 ft (1-2 m) above the active channel. Y1 deposits are found within the geologically active floodplain, not on Finger Rock fan surface. Young debris-flow deposits (unit Y2) are generally found less than 3-5 ft (1-1.5 m) above the active channel, inset below Y1 deposits. Very young debris-flow deposits (unit Y3) are found within or

adjacent to the active channel. These small deposits are limited in extent to near the mountain front. Boulder deposits (unit B) were mapped below Sunset Road to define the general downstream extent of debris flows in Finger Rock Wash. However, two older YI deposits (one too small to map) were found south of mapped B deposits.

Cobblestone Canyon

Cobblestone Canyon (informally named) (Figure 1, map DM-DF-1H) is composed of several small, branching canyons beginning abruptly with steep, fractured and weathered, colluvium-mantled bedrock slopes adjacent to sheer bedrock walls. Drainages are extremely narrow and choked with large boulders. Numerous debris-flow deposits are found above the confluence between the smaller canyons. The active channel within the canyon walls is extremely rocky and narrow, rarely exceeding 15 ft (5 m) across. Outside the canyon walls the channel widens slightly but is still bedrock-lined. Sandy patches are rare and the channel is generally devoid of any loose material. Small patches of vegetation inhabit the channel along fractures and foliations in the bedrock. A deeply dissected, well-rounded fan deposit stretches southward from the mouth of Cobblestone Canyon. Formation of this fan was likely due mainly to deposition of numerous debris flows in the past. The southern extent of mappable debris-flow deposits south of Cobblestone Canyon corresponds roughly with a change in slope on the fan surface. This transition zone may mark a point in the fan-building process where deposition by debris flows was buried by lower gradient stream deposition. The high Cobblestone fan surface is not subject to further deposition below the canyon mouth as all drainages are presently incised up to 200 ft (60 m).

Pleistocene deposits (unit I) are the highest standing boulder deposits in the landscape when located within canyon walls. Here, the upper portions of unit I deposits are lacking fine grained matrix material and consist of large (up to 3 ft [1 m] diameter) boulders resting on other boulders. Below the canyon mouth Pleistocene deposits may be overlain by younger debris-flow and fan deposits. Older YI1 deposits are high-standing debris-flow deposits that are commonly inset into older I deposits. These deposits stand up to 10-12 ft (3-3.5 m) above the active channel. Younger debris-flow deposits are typically inset into YI1 deposits. In narrow bedrock-lined channel settings, YI1 deposits are generally encountered as narrow (less than 15 ft [5 m] across) boulder levees. Large cobbles and boulders are exposed in the steep, near vertical flanks of these deposits. Older YI2 deposits stand 7-10 ft (2-3 m) above the active channel and are often inset into deposits of units I and YI1. YI2 deposits may be significantly vegetated in some areas and devoid of vegetation in others due to the removal of fine matrix sediments by subsequent fluvial reworking and erosion. Overall YI2 deposits are very similar in appearance to YI1 deposits but sit slightly lower in the landscape and exhibit slightly less reddened soils where fine sediment is preserved.

Intermediate debris-flow deposits (unit Y1) are generally found less than 3-7 ft (1-2 meters) above the active channel. These deposits typically do not include boulders greater than 3 ft (1 m) in diameter and some large boulders encountered in inset Y1 deposits may be derived from older, higher-standing YI2 and YI1 deposits. Young debris-flow deposits (unit Y2) are generally found less than 3 ft (1 m) above the active channel. Very young debris-flow deposits (unit Y3) are composed of cobbles to boulders deposited within or adjacent to the active channel. Bouldery stretches of the active channel are sometimes difficult to discern from flanking Y3 deposits. These rocky reaches may be highly eroded or reworked Y3 and higher debris-flow deposits. Elongate cobble- and boulder-dominated deposits are found below the slope break on the Cobblestone canyon fan. Bouldery deposits (unit B) resemble debris-flow levees but may also be cobble and boulder deposits reworked by fluvial processes. When located near the active channel, fine sediments have been removed from B deposits by fluvial

reworking. When located above the active channel, B deposits are often inundated by fine sediments either from initial deposition and subsequent abandonment, soil accumulation, or overbank deposition. Coarse cobble- and boulder-dominated deposits derived from reworked debris-flow deposits (unit C) are found in channel bottoms or forming channel banks. These deposits generally do not exhibit sorting when viewed in channel banks, but also do not exhibit defining debris-flow deposit characteristics. They have probably been winnowed and reworked by fluvial processes.

Pima Canyon

Pima Canyon (Figure 1, map DM-DF-1I) Wash exits the mountain front and flows westward between a large latest Pleistocene to early Holocene fan to the south and bedrock to the north. Approximately ½ mile (1 km) from the fan apex the modern channel turns southward at the interface with a mid-Pleistocene fan. Topography and sedimentary deposits on the latest Pleistocene to early Holocene fan documents channel migration from a more southerly flow to the modern westerly flow. Deposition and build-up of the fan by older debris-flow deposits (units YI1 and YI2) diverted channel flow westward. Younger debris-flow deposits (units Y1, Y2, and Y3) are inset and north of YI fan deposits. Much of the evidence for debris-flow deposits in Pima Canyon is now obscured by residential development.

Pima Wash has a well-defined channel incised 3-10 ft (1-3 m) below a geologically active floodplain (Klawon and others, 1999). Approximately half way between Ina and Orange Grove roads, the floodplain and channel lose definition. William Dickinson (personal communication) speculated that this area might represent a former snout zone. Indeed, evidence of latest Pleistocene to middle Holocene (units YI and Y1) debris-flow deposits was observed in this area, approximately 2.5 miles (4 km) from the mountain front.

Pleistocene deposits (unit I) define the lateral extent of debris flows in Pima Canyon. Pleistocene debris-flow deposits are slightly higher (3-7 ft [1-2 m]) than adjacent YI deposits. Unit I deposits are similar in appearance to YI deposits, but soils are moderately reddened (5YR). YI deposits stand 10-13 ft (3-4 m) above active channels close to the mountains, and 6-10 ft (2-3 m) at the downstream end of mapped deposits. On the fan near the mountain front, YI deposits are divided into higher YI1 and slightly lower YI2 deposits. YI2 deposits are inset 3-7 ft (1-2 m) below YI1 deposits. All YI units are similar in age but the inset relationship of YI1 and YI2 provide clues to channel migration. Farther out from the mountain front, inset relationships between YI1 and YI2 cannot be discerned and are mapped as YI undivided.

Intermediate debris-flow deposits (unit Y1) are generally found less than 3-10 ft (1-3 m) above the active channel, and are highest near the mountain front. Y1 deposits are also found at the downstream extent of mapped debris-flow deposits below Ina Road. Young debris-flow deposits (unit Y2) are generally found less than 2-5 ft (0.5-1.5 m) above the active channel. In general Y2 deposits are inset below Y1 deposits, but some Y2 snouts ($Y2_s$) on-lap and cover Y1 deposits. Very young debris-flow deposits (unit Y3) are limited in extent to near the mountain front and are found within or adjacent to adjacent to the active channel. Boulder deposits (unit B) were used to define the downstream extent of debris flows in Pima Canyon. Cobble and boulder channel deposits (unit C) were mapped in several places along Pima Wash. These deposits typically form 5-7 foot (1.5-2 m) high channel banks. Clasts in these deposits may be weathered and oxidized or relatively fresh looking. Some deposits have stage II+ carbonate coatings.

Pusch Canyon

Pusch Canyon (Figure 1, map DM-DF-1J) is an informally named canyon that drains the south side of Pusch Peak and ridges extending to the south and to the west. Multiple drainages coalesce into one active channel that curves westward to flow on or near the bedrock/alluvial interface. Although most of the channel within the mapped area is mantled with alluvium and debris-flow deposits, bedrock is occasionally exposed in the channel, forming 6-10 foot (2-3 m) bedrock steps. Topography and sedimentary deposits provide evidence for former channels flowing directly south. Deposition and build-up of older debris-flow deposits (YI) blocked flow south forcing flow westward. Younger debris-flow deposits are inset and west of YI deposits. Evidence of debris-flow deposits were not observed below elevation 2,800 ft (850 m) at the Coronado National Forest boundary. Latest Pleistocene to early Holocene (YI) debris-flow deposits may also have been present south of Magee Road; evidence is now obscured by residential development.

One Pleistocene deposit (unit I) was observed in the mapped area, in the south channel bank, near the western extent of observed debris-flow deposits. It is approximately 10 ft (3 m) high, and composed of unsorted cobbles to medium boulders in a reddened (5YR) fine-grained matrix with up to 7 ft (2 m) of stage III to IV carbonate accumulation. This deposit was covered and capped with late Pleistocene (Ql) fine-grained alluvial fan deposits (Klawon and others, 1999). Older YI1 and YI2 debris-flow deposits are the highest standing debris-flow deposits in Pusch Canyon and are up to 10-13 ft (3-4 m) above the active channel. YI1 and YI2 deposits are of similar age but YI2 deposits are inset 3-7 ft (1-2 m) below YI1 deposits. YI1 deposits trend southward while YI2 deposits trend to the southwest illustrating the diversion of flow as sediment accumulated. Intermediate debris-flow deposits (unit Y1) are generally found less than 3-7 ft (1-2 m) above the active channel near the mountain front. Farther west along the channel Y1 deposits may be 6-10 ft (2-3 m) above the active channel. Y1 deposits trend parallel to the current flow of the channel. Young debris-flow deposits (unit Y2) are within 3-5 ft (1-1.5 m) of the active channel, inset below Y1 deposits. In general these deposits do not have fine-grained sediment between clasts except where influenced by vegetation. One such area is a large snout zone along the channel in the middle of the mapped area which has been invaded by buffelgrass. Very young debris-flow deposits (unit Y3) are found within or adjacent to the active channel and limited in extent to near the mountain front.

Linda Vista

Linda Vista Canyon (Figure 1, map DM-DF-1K) is an informally named, small, steep canyon that drains the northwest side of Pusch Peak. A large waterfall separates the upper watershed, where the channel is cut into bedrock, from a lower channel reach that is lined with bouldery debris-flow deposits. Below the waterfall, the channel is in a valley confined by bedrock slopes and ridges of older coarse deposits. The width of the valley bottom generally increases downstream. A major expansion in valley width and decrease in valley confinement about 650 ft (200 m) south of the Coronado National Forest boundary is the approximate apex of an alluvial fan that extends downslope to the north and northwest. The upper part of this fan in the valley mouth is dominated by coarse boulder debris-flow deposits. Much of the lower part of the fan has been obscured by residential development. Where the fan surface is not obscured to the northwest, the lower part of the fan consists of older Pleistocene fan deposits (Spencer and Pearthree, 2004). Progressively younger deposits mantle the fan surface closer to the valley mouth.

Pleistocene debris-flow deposits (unit I) were observed in a few localities in the valley bottom and on the lower part of the alluvial fan complex. Older debris-flow deposits (unit YI) are extensive in the wider

parts of the confined valley and are the most extensive deposits on the alluvial fan at the valley mouth. YI deposits are up to 10 ft (3 m) above the active channel in the confined valley, but farther downslope YI deposits are typically only slightly higher than, and in some places are lower than, adjacent younger debris-flow deposits. YI deposits include large boulders (up to 16 ft [5 m] intermediate diameter) in the confined valley. Intermediate (unit Y1) levee and snout deposits are generally less than 7 ft (2 m) above the active channel but are found farther away from the channel than younger deposits. Y1 boulder levees trend roughly parallel to the channel. Y1 deposits are fairly extensive on the alluvial fan and in the confined valley bottom; based on interpretation of 1960 aerial photos, it appears that a Y1 debris-flow snout extended downslope into the "Linda Vista" neighborhood. Young (unit Y2) and very young (unit Y3) deposits probably record debris-flow activity during the past few thousand years. Y2 deposits typically are perched along the margins of the active channel and are inset only slightly below Y1 deposits. Y3 levees, snouts and generic boulder aggregations are found within or immediately adjacent to the active channel. Y3 deposits commonly are sparsely vegetated, but mature vegetation was found in a few places on Y3 levees and snouts, which implies that they are not historical debris flows. The downstream-most Y3 snout deposits are about 50 ft (15 m) south of the Coronado National Forest boundary.

Numerical Age Dating

Radiocarbon Dates

Two organic carbon samples were collected from Santa Catalina Mountain front debris-flow deposits for ^{14}C (radiocarbon) analysis. In general, datable organic carbon was sparse in debris-flow deposits, probably due to high decomposer activity by termites and other species. The sample that we believed to have the best association with a prehistoric debris flow was collected from Finger Rock Canyon in a small debris-flow levee approximately 3 ft (1 m) above the current bed of the channel. This sample (GX-32841), which consisted of small twigs trapped between boulders, yielded a radiocarbon date of 570±100 years before present. Using the calibration with tree-ring ages, this corresponds to a calendar age range of AD 1251-1518. The second radiocarbon sample (GX-32840), which was collected from the carcass of a saguaro (*Carnegiea gigantea*) that appeared to be killed by a recent debris flow in Pima Canyon, yielded a modern age of 116.14±1.30% of modern ^{14}C activity (see Ely and others, 1992), which corresponds to the early 1950s.

Cosmogenic ^{10}Be Dates

The results of the cosmogenic ^{10}Be dating of debris-flow deposits along channels issuing from the southern Santa Catalina Mountains appears in Table 2 and on the maps accompanying this report. These results show considerable uncertainty in ages, both for individual debris-flow deposits and with respect to the stratigraphic position (surfaces in stratigraphically younger positions have older ^{10}Be ages). In general, the dates indicate that the highest surfaces along Pima, Finger Rock, and Soldier Canyons are of late Pleistocene age, but they provide little resolution within this age range for these surfaces.

The ^{10}Be ages within some surfaces diverge considerably. For example, ages for four boulders from surface L2 at Finger Rock Canyon range from 6,800 to 33,500 years before present (Table 2). The ages are clearly problematic given the stratigraphic constraints; for example, surface L1 at Pima Canyon has ages ranging from 15,200 to 57,600 years before present, and the stratigraphically lower and demonstrably younger surface L3 has ages of 27,200 and 27,300 years before present (Table 2).

Table 2. Cosmogenic exposure ages from ^{10}Be analyses for boulders on debris fans from the southern Santa Catalina Mountains, Arizona.

Sample Name	Sample Number	Thickness Scaling Factor	Shielding Factor	Production Rate (atoms/g/yr)	Exposure Age (yr)	Internal Uncertainty[1] (yr)	External Uncertainty[2] (yr)
Finger Rock L1	070108-01	0.9676	0.9974	8.55	11,100	46	960
Finger Rock L1	070108-02	0.9676	0.9974	8.55	12,100*	241	1,080
Finger Rock L1	070108-02	0.9676	0.9974	8.55	12,000*	57	1,050
Finger Rock L2	070108-04	0.9676	0.9974	8.52	11,000	54	960
Finger Rock L2	070108-05	0.9676	0.9974	8.51	26,400	93	2,300
Finger Rock L2	070108-06	0.9676	0.9974	8.50	6,800	25	600
Finger Rock L2	070108-07	0.9676	0.9974	8.51	33,500	91	2,930
Finger Rock L3	070108-09	0.9676	0.9974	8.48	13,400	49	1,160
Finger Rock L3	070108-10	0.9519	0.9974	8.69	9,229	350	720
Finger Rock L3	070108-11	0.9519	0.9974	8.36	18,500	61	1,610
Finger Rock L4	070108-16	0.9519	0.9974	8.67	4,516	250	400
Finger Rock L4	070108-17	0.9519	0.9974	8.67	7,502	390	640
Finger Rock L4	070108-18	0.9519	0.9974	8.67	14,730	600	1,200
Pima Canyon L1	070109-01	0.9676	0.9993	8.24	15,200*	511	1,420
Pima Canyon L1	070109-01	0.9597	0.9993	8.18	16,200*	53	1,410
Pima Canyon L1	070109-03	0.9676	0.9993	8.24	52,000*	1,000	4,670
Pima Canyon L1	070109-03	0.9836	0.9993	8.38	57,600*	143	5,060
Pima Canyon L1	070109-04	0.9676	0.9993	8.25	28,700	89	2,500
Pima Canyon L2	070109-06	0.9597	0.9991	8.17	12,000	57	1,050
Pima Canyon L2	070109-07	0.9756	0.9991	8.31	12,200	35	1,060
Pima Canyon L3	070109-10	0.9756	0.9991	8.46	7,444	330	610
Pima Canyon L3	070109-11	0.9756	0.9991	8.44	27,200	1,200	2,200
Pima Canyon L3	070109-12	0.9519	0.9991	8.13	27,300	376	2,410
Pima Canyon L3	070109-14	0.9756	0.9991	8.46	8,556		
Sabino DF8 Boulder 1	070110-21	0.9676	0.9706	8.30	8,400*	164	740
Sabino DF8 Boulder 1	070110-21	0.9676	0.9706	8.30	16,300*	218	1,430
Sabino DF8 Boulder 2	070110-23	0.9676	0.9232	7.86	26,100	76	2,280
Soldier Canyon L1	070111-01	0.9597	0.9958	8.01	27,000	95	2,360
Soldier Canyon L1	070111-03	0.9676	0.9962	8.07	59,500	148	5,230
Soldier Canyon L3	070111-08	0.9676	0.9962	8.19	28,600	75	2,500
Soldier Canyon L3	070111-09	0.9676	0.9881	8.12	27,900	74	2,440
Soldier Canyon L3	070111-10	0.9676	0.9962	8.18	38,800	606	3,450
Soldier Canyon L5	070111-16	0.9676	0.9962	8.42	23,800	1,070	1,900

[1]Internal uncertainty is the ability of the lab to make the measurement.

[2]External uncertainty is the variation in production rate and other factors needed to complete the calculation, such as variation in lat-long-shielding.

* These are replicate samples to check for consistency among dates with sample preparation in different laboratories.

Insufficient beryllium was present to yield a current in the AMS.

The sample collected from the unnamed drainage at tram stop 8 in Sabino Canyon (DF8; Table 2) indicates that the cobbles had a calculated age of more than 800,000 years even though they were transported to the location where they were deposited in 2006. These results indicate that the assumption of shielding for particles at initiation sites in the Santa Catalina Mountains is bad and (or) stable bedrock outcrops long exposed to cosmic radiation failed during the 2006 event.

DISCUSSION

All fifteen canyons mapped along the south and west sides of the Santa Catalina Mountains had evidence of past debris flows (Figure 1, Map Sheets 1-11). The highest and most extensive debris-flow deposits at all of the canyon mouths probably date to the latest Pleistocene to early Holocene. In most canyons two major pulses of latest Pleistocene – early Holocene debris-flow activity were identified based on inset relationships of the deposits. Inset relationships of similarly aged deposits and current channel configurations provide information about channel migration across fan surfaces, and channel incision and entrenchment. Early to latest Holocene debris-flow deposits were also found in all canyons. These younger debris-flow deposits are generally more limited in extent than older deposits. However, in Soldier Canyon, the 2006 debris-flow deposited boulders near the downslope extent of older debris-flow deposits.

Coarse boulder deposits were found surprisingly far from the mountain front in Esperero, Pontatoc, Finger Rock, and Pima Canyons. These deposits exhibit surface characteristics similar to latest Pleistocene to early Holocene (YI or Y1) debris-flow deposits near the canyon mouths. In the four canyons with these distal deposits the geologically active floodplain is confined between older Pleistocene to Tertiary sediments. While these deposits have likely been reworked by subsequent large floods, they were probably emplaced by multiple debris flows or pulses that broke through existing debris-flow deposits thereby re-initiating transport downstream. Debris flows can be re-initiated if a subsequent pulse or a later flood breaks through a snout effectively acting like a dam break. It is possible these deposits are solely a result of floods flows reworking material from debris-flow deposits higher in the system. However, while floods can move large bedload in increments, debris flows have much more competence and capacity to move larger material cohesively. Flow modeling may provide some answers as to the likelihood that these deposits are flood related rather than debris-flow related. Regardless of the type of flow - flood or debris flow - reworking these coarse, boulder deposits requires large magnitude events and therefore presents potential risks. However, it is unlikely debris flows in these canyons have traveled such distances in the past few thousand years.

Mapped debris-flow deposits represent a minimum number of deposits for several reasons. Each mapped deposit may have formed as a result of multiple pulses from a single debris flow or numerous successive debris flows. Not all Holocene debris-flow deposits are preserved due to the active nature of the channel environment and erosion and deposition in subsequent debris flows. Many debris-flow deposits are likely overlain by more recent deposition and are not visible at the surface. Finally, bouldery reaches of the channel may be attributed to either reworked debris-flow sediments or heavily eroded debris-flow lobes. Based on the local topography and channel -bank exposures of underlying unsorted to poorly sorted sediment, coarse young deposits at the canyon mouths of each study canyon record significant debris-flow activity. The youngest of these deposits in each canyon were probably emplaced in the past few thousand years. Thus, some potential remains for debris-flows activity near the mountain front, and there may be some risk to developed areas and infrastructure.

Radiocarbon dating of two debris-flow deposits resulted in one age of 550 years before present from Finger Rock Canyon and a modern age from Pima Canyon. Boulders from several levees in Soldier, Sabino, Finger Rock and Pima Canyons were also dated using ^{10}Be. The divergence of ages on surfaces constructed of debris-flow deposits strongly suggests problems with application of ^{10}Be cosmogenic dating to the problem of debris-flow ages in the Santa Catalina Mountains. These problems likely stem from substantial prior exposure history and lack of shielding prior to transport, whether the debris flow occurred in the late Pleistocene or in 2006. Because any of these problems would result in an exposure age estimate that is older than the time the deposits were emplaced in their current positions, the youngest exposure age dates are likely to most closely approximate deposit age.

Numeric age dating did provide a general corroboration with the relative age dating of the mapped debris-flow deposits, although the degree of correlation varied between canyons. For example, the youngest ^{10}Be exposure dates and relative age estimates from YI1, YI2, and Y1 deposits in Finger Rock Canyons correlate quite well. Generally similar exposure age estimates were obtained for debris-flow deposits in Pima Canyon. Conversely , all ^{10}Be dates from Soldier Canyon were surprisingly older than expected from geologic mapping and relative age dating.

Based on data from geologic mapping and from numeric age dating techniques, average recurrence intervals between debris flows in individual canyons may be on the order of thousands of years. The largest and most extensive deposits in all of the mapped canyons occurred during the late Pleistocene to the early Holocene. The youngest debris-flow deposits are limited in size and extent. Nevertheless, as seen in 2006, the potential exists for debris flows to exit the mountain front into developed areas when they do occur.

ACKNOWLEDGEMENTS

Many people contributed to the development of this report. Funding for this research was provided by Pima County Regional Flood Control District and the Arizona Geological Survey. This work was conducted in cooperation of the United States Geological Survey. Pima County Regional Flood Control District provided aerial photographs and digital orthophotographic images. We thank the many home owners, home owner associations, and the Coronado National Forest for providing access for mapping. Colby Bowser, from the Office of Supervisor Ann Day, was especially helpful in obtaining access permissions. Chris Magirl and Peter Griffiths of the USGS, and Evan Canfield, Mark Krieski, and Akitsu Kimoto of Pima County Regional Flood Control district engaged in many discussions about this work and provided thoughtful reviews that substantially improved this manuscript. We thank Bill Dickinson, professor emeritus in the University of Arizona Geosciences Department, for suggesting we expand our mapping efforts to areas below Ina Road in Pima Canyon. All maps were designed and produced by Ryan Clark.

REFERENCES

Anderson, R.S., Repka, J.L., and Dick, G.S., 1996, Explicit treatment of inheritance in dating depositional surfaces using in situ 10 Be and 26 Al: Geology, v. 24, no. 1, p. 47-51.

Anderson, S.A., and Sitar, N., 1995, Analysis of Rainfall-Induced Debris Flows: Journal of Geotechnical Engineering, v. 121, no. 7, p. 544.

Bagnold, R.A., 1954, Experiments on a Gravity-Free Dispersion of Large Solid Spheres in a Newtonian Fluid under Shear: Proceedings of the Royal Society of London Series A-Mathematical and Physical Sciences, v. 225, no. 1160, p. 49-63.

Balco, G., Stone, J.O., Lifton, N.A., and Dunai, T.J., 2008, A complete and easily accessible means of calculating surface exposure ages or erosion rates from ^{10}Be and ^{26}Al measurements: Quaternary Geochronology, v. 3, no. 3, p. 174-195.

Bierman, P.R., Gillespie, A.R., and Caffee, M.W., 1995, Cosmogenic Ages for Earthquake Recurrence Intervals and Debris Flow Fan Deposition, Owens Valley, California: Science, v. 270, no. 5235, p. 447-450.

Birkland, P.R., 1999, Soils and Geomorphology (Third ed.): New York, Oxfod University Press, 430 p.

Bookhagen, B., 2007, Chemical separation of Al and Be from quartz-bearing rocks: Stanford, California, Stanford University, Department of Geosciences, p. 48.

Cannon, S.H., 2001, Debris-flow generation from recently burned watersheds: Environmental and Engineering Geoscience, v. 7, no. 4, p. 321-341.

Cannon, S.H., Bigio, E.R., and Parise, M., 2002, Debris-flow initiation processes from basins recently burned by wildfire, Western USA, Abstracts with Programs - Geological Society of America, Geological Society of America, p. 469.

Cannon, S.H., and Gartner, J.E., 2005, Wildfire-related debris flow from a hazards perspective, *in* Jakob, M., and Hungr, O., eds., Debris-flow hazards and related phenomena: Berlin, Springer, p. 363-385.

Cerling, T.E., Webb, R.H., Poreda, R.J., Rigby, A.D., and Melis, T.S., 1999, Cosmogonic (super 3) He ages and frequency of late Holocene debris flows from Prospect Canyon, Grand Canyon, USA: Geomorphology, v. 27, no. 1-2, p. 93-111.

Costa, J.E., 1984, Physical geomorphology of debris flows, *in* Costa John, E., and Fleisher, P.J., eds., Developments and applications of geomorphology.: Berlin, Federal Republic of Germany, Springer-Verlag, p. 268-317.

De Wrachien, D., 2006, Introduction to Special Section 3: Debris and hyperconcentrated flows, in First International Conference on Monitoring, Simuation, Prevention and Remediation of Dense and Debris Flows, Rhodes, Greece, WIT Press, p. 131-134.

Ely, L.L., Webb, R.H., and Enzel, Y., 1992, Accuracy of post-bomb 137Cs and 14C in dating fluvial deposits: Quaternary Research, v. 38, no. 2, p. 196-204.

Federal Emergency Management Agency, 2008, Landslide and Debris Flow (Mudslide), http://www.fema.gov/hazard/landslide/index.shtmLan.

Gartner, J.E., Cannon, S.H., Santi, P.M., and DeWolfe, V.G., 2005, Relations between debris-flow volumes generated from recently burned basins and basin morphology, triggering storm rainfall and material properties, Abstracts with Programs - Geological Society of America, Geological Society of America, p. 36.

Gartner, J.E., Cannon, S.H., Santi, P.M., and Dewolfe, V.G., 2007, Empirical models to predict the volumes of debris flows generated by recently burned basins in the Western U.S: Geomorphology, v. doi:10.1016/j.geomorph.2007.02.033.

Glenn, N.F., Streutker, D.R., Chadwick, D.J., Thackray, G.D., and Dorsch, S.J., 2006, Analysis of LiDAR-derived topographic information for characterizing and differentiating landslide morphology and activity: Geomorphology, v. 73, no. 1-2, p. 131-148.

Gosse, J.C., and Phillips, F.M., 2001, Terrestrial in situ cosmogenic nuclides: theory and application: Quaternary Science Reviews, v. 20, no. 14, p. 1475-1560.

Hungr, O., 2005, Classification and terminology, *in* Jakob, M., and Hungr, O., eds., Debris-flow hazards and related phenomena: Berlin, Springer.

Iverson, R.H., 1997, The physics of debris flows: Reviews of Geophysics, v. 35, no. 3, p. 245-296.

Iverson, R.M., Logan, M., Denlinger, R.P., and LaHusen, R.G., 2005, Transformation of water floods to debris flows; large-scale experiments, Abstracts with Programs - Geological Society of America, Geological Society of America, p. 35.

Iverson, R.M., Reid, M.E., and LaHusen, R.G., 1997, Debris-flow mobilization from landslides: Annual Review of Earth and Planetary Sciences, v. 25, p. 85-138.

Iverson, R.M., and Vallance, J.W., 2001, New views of granular mass flows: Geology, v. 29, no. 2, p. 115-118.

Klawon, J.E., Dickinson, W.R., and Pearthree, P.A., 1999, Surficial Geology and Geologic Hazards of the Northern Tucson Basin, Pima County, Arizona, Tucson North and Sabino Canyon Quadrangles: Arizona Geological Survey, scale 1:24,000.

Lenzi, M.A., 2006, Research developments in debris flow monitoring, modelling and hazard assessment in Italian mountain catchments, in First International Conference on Monitoring, Simulation, Prevention and Remediation of Dense and Debris Flows, Rhodes, Greece, WIT Press, p. 135-145.

Libby, W.F., Anderson, E.C., and Arnold, J.R., 1949, Age Determination by Radiocarbon Content: World-Wide Assay of Natural Radiocarbon: Science, v. 109, no. 2827, p. 227-228.

Magirl, C.S., Webb, R.H., Griffiths, P.G., Schaffner, M., Shoemaker, C., Pytlak, E., Yatheendradas, S., Lyon, S.W., Troch, P.A., Dislets, S.L.E., Goodrich, D.C., Unkrich, C.L., Youberg, A., and Pearthree, P.A., 2007, Impacts of recent extreme Arizona Storms: Eos, Transactions, American Geophysical Union, v. 88, no. 17.

Melis, T.S., Webb, R.H., and Griffiths, P.G., 1997, Debris flows in Grand Canyon National Park; peak discharges, flow transformations, and hydrographs, *in* Chen Cheng, l., ed., First international conference on Debris-flow hazards mitigation; mechanics, prediction and assessment.: New York, NY, American Society of Civil Engineers, p. 727-736.

Menges, C.M., Taylor, E.M., Workman, J.B., and Jayko, A.S., 2001, Regional surficial-deposit mapping in the Death Valley area of California and Nevada in support of ground-water modeling, *in* Machette, M.N., Johnson, M.L., and Slate, J.L., eds., Quaternary and late Pliocene geology of the Death Valley region: recent observations on tectonics, stratigraphy, and lake cycles (Guidebook for the 2001 Pacific Friends of the Pleistocene Field Trip): Reston, VA, US Geological Survey Open-File Report 01-0051 (http://pubs.usgs.gov/of/2001/ofr-01-0051/). p. H151-H166.

Meyer, G.A., Pierce, J.L., and Wood, S.H., 2001, Fire-induced sedimentation in Rocky Mountain conifer forests, Abstracts with Programs - Geological Society of America, Geological Society of America, p. 14.

Montgomery, D.R., and Buffington, J.M., 1997, Channel-reach morphology in mountain drainage basins: Geol Soc Am Bull, v. 109, no. 5, p. 596-611.

O'Brien, J.S., Julien, P.Y., and Fullerton, W.T., 1993, Two-Dimensional Water Flood and Mudflow Simulation: Journal of Hydraulic Engineering, v. 119, no. 2, p. 244-261.

Pearthree, P.A., 2004, Geologic Map of the Huachuca City 7½' Quadrangle, Cochise County, Arizona: Arizona Geological Survey, scale 1:24000.

Pearthree, P.A., and Youberg, A., 2006, Recent debris flows and floods in southern Arizona: Arizona Geology, v. 36, no. 3, p. 1-5.

Pierson, T.C., 2005a, Distinguishing between debris flows and floods from field evidence in small watersheds: Reston, VA, U. S. Geological Survey, 4 p.

Pierson, T.C., 2005b, Hyperconcentrated flow; transitional process between water flow and debris flow, *in* Jakob, M., and Hungr, O., eds., Debris-flow hazards and related phenomena: Berlin, Springer.

Pierson, T.C., and Costa, J.E., 1987, A rheologic classification of subaerial sediment-water flows, *in* Costa John, E., and Wieczorek Gerald, F., eds., Debris flows/ avalanches; process, recognition, and mitigation: Boulder, Geological Society of America, p. 1-12.

Rowbotham, D., Scally, F.D., and Louis, J., 2005, The Identification of Debris Torrent Basins Using Morphometric Measures Derived within a Gis: Geografiska Annaler, Series A: Physical Geography, v. 87, no. 4, p. 527-537.

Santi, P.M., deWolfe, V.G., Higgins, J.D., Cannon, S.H., and Gartner, J.E., 2007, Sources of debris flow material in burned areas, Geomorphology, v. doi: 10.1016/j.geomorph.2007.02.022.

Santi, P.M., deWolfe, V.G., Higgins, J.D., Cannon, S.H., and Gartner, J.E., 2008, Sources of debris flow material in burned areas: Geomorphology, v. 96, no. 3-4, p. 310-321.

Sosio, R., Crosta, G.B., and Frattini, P., 2007, Field observations, rheological testing and numerical modelling of a debris-flow event: Earth Surface Processes and Landforms, v. 32, no. 2, p. 290-306.

Spencer, J.E., and Pearthree, P.A., 2004, Geologic map of the Oro Valley $7^{1}/_{2}$' Quadrangle and the Pusch Peak area, northeastern Pima County, Arizona, scale 1:24000.

Stock, J.D., and Dietrich, W.E., 2006, Erosion of steepland valleys by debris flows: Geol Soc Am Bull, v. 118, no. 9-10, p. 1125-1148.

Takahashi, T., Satofuka, Y., and Chishiro, K., 1997, Dynamics of debris flows in the inertial regime, *in* Chen Cheng, l., ed., First international conference on Debris-flow hazards mitigation; mechanics, prediction and assessment.: New York, NY, United States, American Society of Civil Engineers, p. 239-248.

Tarboton, D.G., 2005, Terrain Analysis Using Digital Elevation Models (TauDEM): Logan, Utah State University.

Terranova, O., Antronico, L., and Gulla, G., 2007, Landslide triggering scenarios in homogeneous geological contexts: The area surrounding Acri (Calabria, Italy): Geomorphology, v. 87, no. 4, p. 250-267.

Tucker, G., and Bras, R., 1998, Hillslope Processes, Drainage Density, and Landscape Morphology: Water Resources Research, v. 34, no. 10, p. 2751-2764.

Tucker, G.E., Catani, F., Rinaldo, A., and Bras, R.L., 2001, Statistical analysis of drainage density from digital terrain data: Geomorphology, v. 36, no. 3-4, p. 187-202.

Webb, R., Griffiths, P.G., and Melis, T.S., 2005, Initiation of debris flows in bedrock canyons in the Colorado River, *in* Anonymous, ed., Geological Society of America, 2005 annual meeting.: Geological Society of America (GSA). Boulder, CO, United States. 2005.

Webb, R.H., Magirl, C.S., Griffiths, P.G., and Boyer, D.E., 2008, Debris flows and floods in southeastern Arizona from extreme precipitation in late July 2006: Magnitude, frequency, and sediment delivery: United States Geological Survey.

Webb, R.H., Melis, T.S., Griffiths, P.G., Elliott, J.G., Cerling, T.E., Poreda, R.J., Wise, T.W., and Pizzuto, J.E., 1999, Lava Falls Rapid in Grand Canyon: effect of late Holocene debris flows in the Colorado River: U. S. Geological Survey, 90 p.

Wieczorek, G.F., and Glade, T., 2005, Climatic factors influencing occurrence of debris flows, *in* Jakob, M., and Hungr, O., eds., Debris-flow hazards and related phenomena: Berlin, Federal Republic of Germany, Springer.

Wilford, D.J., Sakals, M.E., Innes, J.L., Sidle, R.C., and Bergerud, W.A., 2004, Recognition of debris flow, debris flood and flood hazard through watershed morphometrics: Landslides, v. 1, no. 1, p. 61-66.

Wohl, E., 2000, Mountain rivers: Washington, DC, American Geophysical Union, v. Water Resources Monograph, 320 p.

Wohl, E.E., and Pearthree, P.A., 1991, Debris flows as geomorphic agents in the Huachuca Mountains of southeastern Arizona: Geomorphology, v. 4, no. 3-4, p. 273-292.

Wolkowinsky, A.J., and Granger, D.E., 2004, Early Pleistocene incision of the San Juan River, Utah, dated with 26Al and 10Be: Geology, v. 32, no. 9, p. 749-752.

GEOLOGIC TIMESCALE

Geologic Timescale used in this report. Ages are in thousands of years before present (Ka).

Time Periods	Age (Ka)
Late Holocene	0-4
Middle Holocene	4-8
Early Holocene	8-11
Pleistocene Latest	11-22
Pleistocene Late	11-125
Pleistocene Middle	125-750
Pleistocene Early	750-2,000

GLOSSARY

Alluvial Fan Here we use a geomorphic definition that has no legal flood-hazard designation. An alluvial fan is a depositional surface emanating from a channel that debouches from a mountain range or other incised/confined drainage or channel system. Alluvial fans are constructed from fluvially transported sediment (for example, streamflow and (or) debris-flow deposits) and may contain a small amount of colluvium derived from rock avalanches or rockfalls that occur near their apices. This definition does not distinguish between alluvial fans with fan-head entrenchment or fully incised channels and those with little or no channel definition (or distributary channels) that are more common in more tectonically active areas than southern Arizona.

Annual Flood Series A time series of the annual peak discharges for a streamflow gaging station that is used in flood-frequency analysis.

Boulder Train A crudely linear group of boulders that may or may not be deposited during a debris flow upstream or downstream of a flow obstruction. Typically flow obstructions include large immobile boulders and trees. Boulder trains that form downstream from flow obstructions tend to be deposited by streamflow, while boulder trains that form upstream from flow obstructions or along the margins of flow tend to be deposited by debris flows.

Colluvium Poorly sorted sediment that accumulates from rockfall or overland flow, typically on steep slopes. Coarse colluvium may accumulate during discrete rockfalls or avalanches or may accrue over long periods of time from episodic additions.

Contributing Area The upslope area above any given point in a basin through which surface water flows.

Cosmogenic Dating The use of isotopic extraction and measurement techniques to estimate the age of particles at the Earth's surface from the natural rate of accumulation of certain isotopes generated through spallation processes caused by cosmic-ray bombardment. Cosmogenic dating directly dates particles in a geologic deposit, but uncertainties may arise from prior exposure to cosmic radiation (i.e., the particle moved from a position on the Earth's surface to a different exposed position) or through erosion. Cosmogenic ^{10}Be dating, summarized here, theoretically can be used to date deposits millions of years old but in practice is limited by the erosion rate of particles and their deposits.

Debris Flow A two-phase fluid of less than 40% water and more than 60% sediment, generally very poorly sorted, that typically results from slope failures in the desert Southwest. Debris flows are considered to be non-Newtonian flows that are dominated by particle-particle friction.

Debris-Flow Deposit Typically, a poorly sorted deposit of particles along a watercourse. Debris-flow deposits can be difficult to distinguish from streamflow deposits or colluvium, but several characteristics can be definitive: (1) the presence of poorly-sorted sediment with a surface subparallel to a channel, (2) the general lack of strongly imbricated particles in the deposit, (3) the presence of boulder trains extending upstream from an obstruction, (4) large particles (e.g., boulders) resting on a bed of fine-grained sediment and not in contact with other large particles within a deposit, (5) the general lack of stratification in deposits. Many of these characteristics may also be present in hyperconcentrated deposits.

Holocene The Holocene generally is considered to be the last 11,000 years of geologic time.

Hyperconcentrated Flow Deposits These deposits, while recognizable from certain stratigraphic characteristics, result from only vaguely known sediment transport processes that may result from pulses of debris flow and (or) runout facies downstream of debris-flow deposition, or they may result from flash-flood sediment transport unrelated to debris flows. Sediment concentration in hyperconcentrated flow generally is in the 40-60% range by weight. When associated with debris flows, hyperconcentrated flow deposits have a characteristic arrangement of stratigraphic layers, which can be relatively thin, that show alternating deposition of poorly sorted sediment (but with smaller particles) with relatively well sorted sand or gravel lenses.

Imbrication Three-dimensional arrangement of pebbles, cobbles and boulders in a sedimentary deposit that indicates either streamflow deposition or reworking by streamflow. Imbricated deposits may appear to be flat-lying and overlapping as if tiled. Gravel particles dip upstream, opposite to the flow direction.

Landslide This term is somewhat ambiguous when applied to desert environments. In more humid environments, a landslide is a deep-seated slope failure of large spatial extent that typically moves along a saturated failure plane fed by ground water; the overlying sediments

may or may not be saturated. To avoid confusion, we typically refer to the saturated shallow failures that occurred in July 2006 using the generic slope failure term.

Levee In this case, a debris-flow deposit along the margin or center of a channel that has a characteristic form and poorly sorted particles. Boulders generally are the most obvious particles in a debris-flow levee. Lateral levees typically form along the margins of channels; medial levees typically occur in the center of channels.

Matrix deposits Debris-flow matrix deposits represent a reasonably intact sample of the range of particles transported during a debris flow, at least at the time of deposition during the event.

Mudflow A debris flow with a high (typically >40%) content of fine-grained sediment and minimal coarse particles. Mudflows seldom occur in Arizona and none occurred during the 2006 event.

Pleistocene The Pleistocene represents the period of geologic time from 2 million to 11,000 years before present. The latest Pleistocene is 22,000 to 11,000 years before present in our usage.

Quaternary The Quaternary period of geologic time is the past 2 million years and includes the Pleistocene and the Holocene.

Radiocarbon (or ^{14}C) Dating Carbon 14 (^{14}C) is a radioactive isotope with a half-life of 5,200 years that is created by cosmogenic bombardment of nitrogen atoms in the upper atmosphere. Plants and animals accrue ^{14}C in proportion to its concentration in the atmosphere, and after death, ^{14}C decays in organic material, providing a time interval between accrual and the present used to determine an age. ^{14}C measured in geologic deposits has an uncertain association that may create errors in dating.

Recurrence Interval This statistical term, also called a return period, refers to how often, on average, an expected observation will occur in time. Although this term is used for hazard prediction, and technically the 100-year flood is an event with a 1:100 probability of occurring in the next year, recurrence interval is also used to describe a recent event in terms of its past rate of occurrence and is useful in describing the magnitude and frequency of meteorological and hydrological events.

Reworking Alteration in the particle size and form of a deposit after its deposition. Recessional streamflow that follows a debris flow may entrain fine-grained sediment and alter the geometric arrangement of larger particles, and these changes may obscure the original deposition mechanism.

Rockfall Typically a failure in bedrock of small spatial extent that rapidly travels downslope as isolated particles, not a coherent mass.

Scarps (head scarps) An abrupt, steep slope of soil where slope failure occurred.

Slope Failure A generic term that applies to a wide range of sediment delivery mechanisms from steep slopes to channels that usually involves rapid entrainment of relatively large amounts of sediment into water flow. Types of slope failures range from landslides, which are relatively slow moving, to avalanches and rockfalls, which move extremely quickly. Here, we refer to shallow-seated slope failures, which are of limited spatial extent and have thicknesses of less than 10 feet and typically less than 3 feet.

Snout Terminal deposits of a debris flow that typically are poorly sorted and contain large boulders.

Streamflow Newtonian flow that typically contains less than 40% sediment.

Streamflow flood Although any flow in an ephemeral channel during a rising stage might be considered a flood, here we consider a flood to be either the largest flow that occurs in a year or a group of flows that are extremely high in the recorded history of a watercourse at a gaging station.

Thalweg The deepest part of a channel.